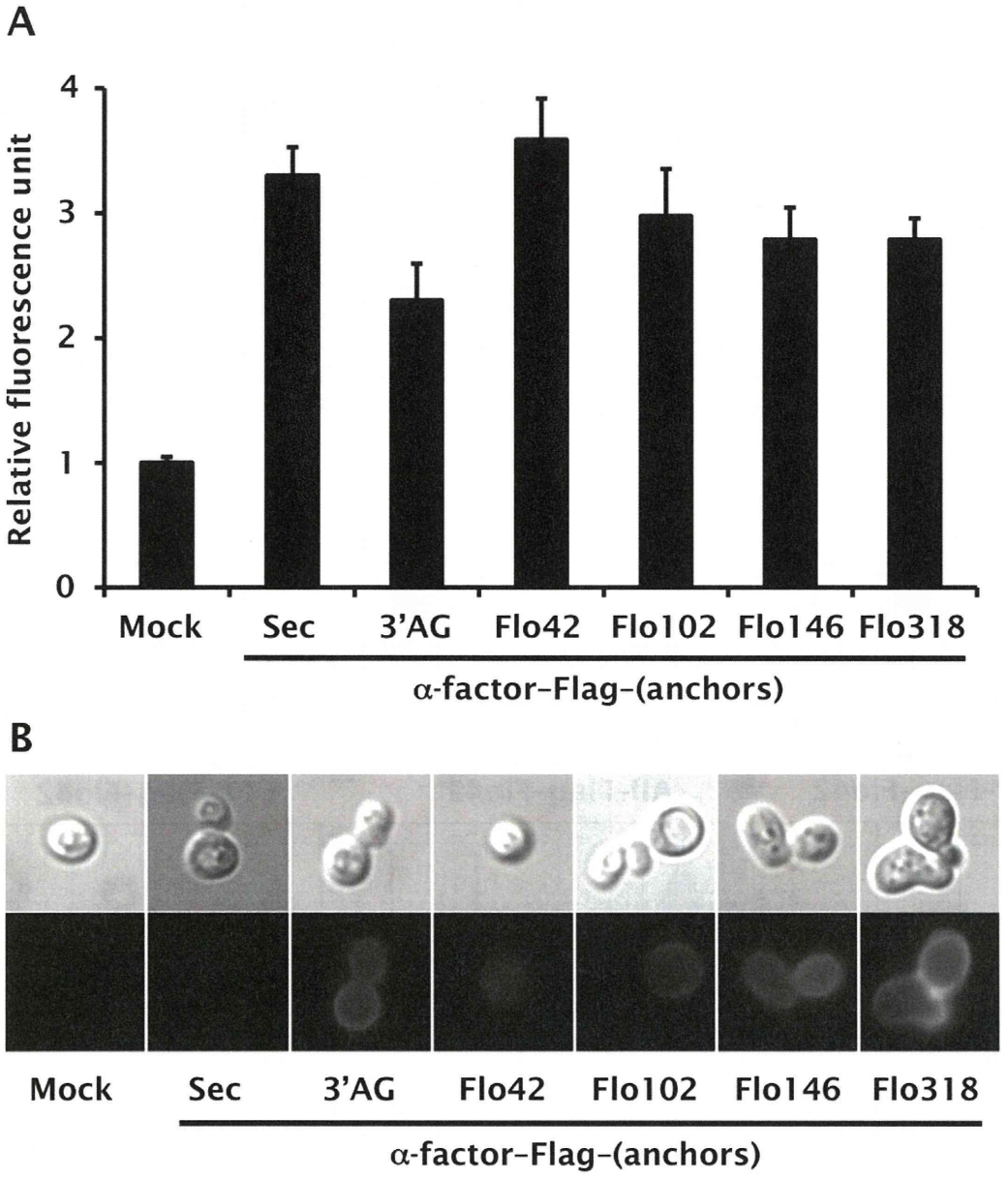

Figure 3. Evaluation of the CWTrAP system using α-factor peptide for yeast endogenous Ste2 receptor. (A) Pheromone signaling assays of α-factor-displaying yeast strains. Error bars represent the standard deviation of three independent experiments. (B) Immunofluorescence staining of α-factor displaying yeast strains. Anti-Flag antibody and Alexa Fluor 546-conjugated secondary antibody were used for detection of secreted α-factor or α-factor-anchor fusion proteins. IMG-4 was used as the host strain. The transformants used in these experiments are listed in Table S3. Sec: free, secreted form of α-factor. AG: C-terminal half of α-agglutinin anchor.
doi:10.1371/journal.pone.0037136.g003

cassette (pMHG-FIG1 [6]) (Figure 6). These results strongly support the feasibility of our conceptual CWTrAP system to identify eligible agonistic peptides for human GPCRs.

Finally, to examine whether the yeast cell wall did indeed trap the autocrine peptide fused to the Flo42 anchor, transformants were analyzed by immunofluorescence staining with anti-Flag primary antibody and Alexa Fluor 594 conjugated secondary antibody (Figure 7). We observed red fluorescence on the cell surfaces of appropriate transformants that expressed Flag Flo42 anchor or S-14 Flag Flo42 fusion proteins. In addition, we only observed a morphology change [29] on cells expressing both SSTR5 HA and S-14 Flag Flo42, supporting our hypothesis that the autocrine S-14 peptide specifically triggered signal transduction via the SSTR5 receptor in the recombinant yeast cells. Thus, we successfully verified that the S-14 autocrine peptide fused to the Flo42 anchor protein was trapped on the yeast cell wall.

In this study, we have demonstrated how a strategy for cell wall trapping of autocrine peptides (CWTrAP system) functions to discern agonistic activity for human GPCRs expressed in yeast

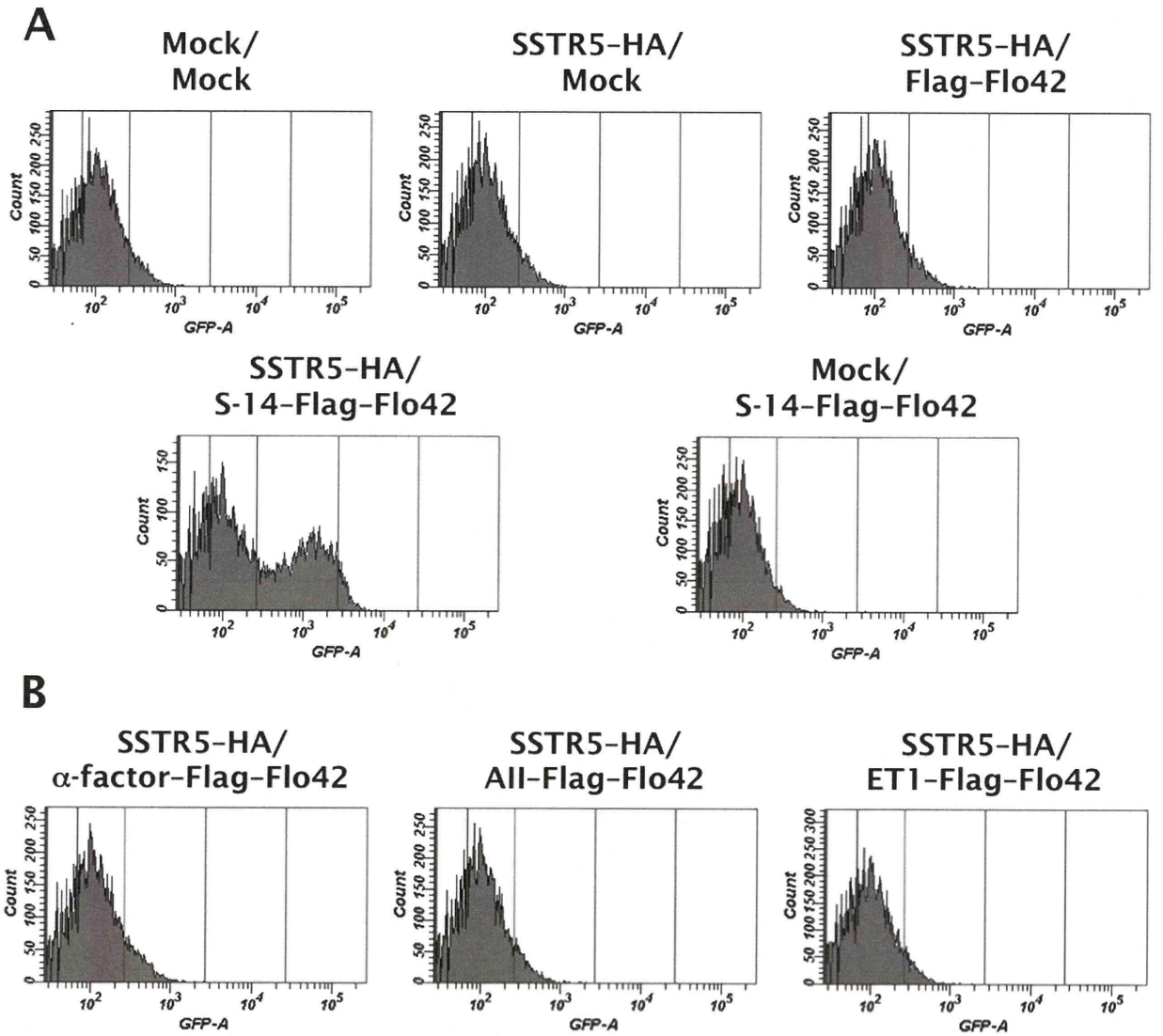

Figure 4. Evaluation of the CWTrAP system using somatostatin peptide for the human SSTR5 receptor. (A) SSTR5 signaling assays of the cyclic somatostatin peptide displaying yeast strain and control strains. (B) SSTR5 signaling assays of non-target peptide displaying yeast strains. IMFD-70 was used as the host strain. The transformants used in these experiments are listed in Table S3. S-14 indicates 14 aa of somatostatin cyclic peptide, α-factor indicates 13 aa of yeast pheromone peptide, AII indicates 8 aa of angiotensin II peptide, and ET1 indicates 21 aa of endothelin-1 peptide.
doi:10.1371/journal.pone.0037136.g004

cells, by using the intramolecular-cross-linked cyclic peptide S-14 and its specific receptor as our model. Our motivation was to selectively track eligible agonistic peptides for human GPCRs by assembling an autonomous signaling complex within individual cells. By combining cell-surface display technology and established yeast combinatorial genetic engineering technology with flow cytometric single-cell screening [30], we aim to identify eligible peptides from peptide libraries. Here, the feasibility of our concept is demonstrated by peptide capture, and subsequent signal transduction, by heterologously-expressed human GPCRs, which prevent the captured peptides from diffusing to surrounding yeast cells and eliciting a false-positive response. Therefore, the captured peptides are successfully presented by yeast cell-surface display technology.

Materials and Methods

Media

Synthetic raffinose (SR) media contained 6.7 g/l yeast nitrogen base without amino acids (YNB) (BD-Diagnostic Systems, Sparks, MD, USA) and 20 g/l raffinose. For SRGC media, 20 g/l galactose and 20 g/l casamino acids (BD-Diagnostic Systems) were added into SR media. Synthetic dextrose (SD) media contained 6.7 g/l YNB and 20 g/l glucose. For SDM71 media, SD media was adjusted to pH 7.1 with 200 mM MOPSO buffer (Nacalai Tesque, Kyoto, Japan). Amino acids and nucleotides (20 mg/l histidine, 60 mg/l leucine, 20 mg/l methionine or 20 mg/l uracil) were supplemented into each medium to provide the relevant auxotrophic components.

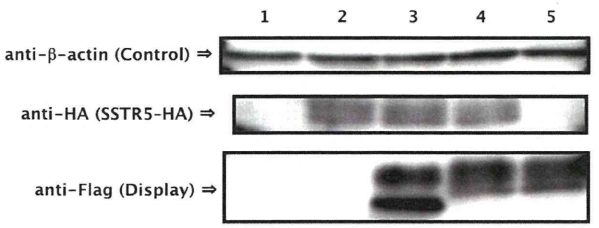

Figure 5. Confirmation of protein expression. Western blots of extracts from somatostatin displaying yeast strains. Lane 1: Mock/Mock, 2: SSTR5/Mock, 3: SSTR5/Flag–Flo42, 4: SSTR5/S-14–Flag–Flo42, 5: Mock/S-14–Flag–Flo42. Anti-β-actin antibody was used as loading control. Anti-HA antibody was used for detection of SSTR5 receptor. Anti-Flag antibody was used for detection of Flag–Flo42 anchor or S-14–Flag–Flo42 fusion proteins. IMFD-70 was used as the host strain. The transformants used in these experiments are listed in Table S3.
doi:10.1371/journal.pone.0037136.g005

Yeast Strains

Yeast strains used for assays were generated from BY4741 [31] as a parental backbone strain and are listed in Table 1. The transformation procedure using linear DNA fragments followed the lithium acetate method [32]. All primers used for the strain constructions are listed in Table S1. The *bar1*Δ alleles that relieve the degradation of α-factor pheromone [33] were conferred to BY4741*far1*Δ (obtained from *Saccharomyces* Genome Deletion Project [34]) by homologous recombination with the amplified *LEU2* fragments, producing the IM-4 strain. The *FUS1-GFP* reporter gene was integrated into the *FUS1* genomic loci of IM-4 with a fragment prepared by digestion of pUC119-FUS1-EGFP-HIS3 [28] with EcoRI and SphI, producing the IMG-4 strain. The P_{FUS1}-*FUS1-GFP* or P_{FIG1}-*GFP* reporter gene was used to monitor signal transduction promoted by stimulating GPCRs in yeast (IMG-4, IMG-50 or IMFD-70 [5]). *far1*Δ alleles were used to avoid G1 arrest and promote cell-cycle progression during signal activation [5,28,35] (IMG-4 and IMFD-70). *sst2*Δ and *ste2*Δ alleles were used to obtain hypersensitivity for ligand stimulation and to inhibit competitive expression of endogenous yeast GPCRs [5,28] (IMG-50 and IMFD-70).

Plasmids

All plasmids used for assays are listed in Table 1. All primers used for plasmid constructions are listed in Table S1. The amplified pre, pro (containing secretion signal sequence, s.s.) and first mature sequences of α-factor peptide including a C-terminal Flag tag and stop codon were inserted into the pESC-URA yeast expression vector (Agilent Technologies, Santa Clara, CA, USA) at the BamHI and XhoI sites, creating pUESCαsf. As the backbone for α-factor-displaying plasmids, pUESCαf and pUESCαf(AG) without stop codons were constructed in essentially the same manner. The amplified genes encoding Flo42, Flo102, Flo146 and Flo318 anchors were inserted into pUESCαf at the XhoI and NheI sites, resulting in pUESCαf-FLO42, -FLO102, -FLO146 and -FLO318, respectively. pUESCαf-AG was produced in a similar procedure by inserting the gene encoding the C-terminal 320 aa of Sag1p (C-terminal half of α-agglutinin anchor, AG) into pUESCαf(AG) at the XhoI and NheI sites. As the backbone for somatostatin-displaying plasmids, we constructed pGK426-tgFLO42 by inserting the amplified *FLO42* anchor gene with *FLAG* at the N-terminus into pGK426 at the SalI and BglII sites [36]. The DNA fragment containing s.s. of α-factor and S-14 mature peptide was amplified by overlapping PCR and inserted into pGK426-tgFLO42 at the NheI and SalI sites, producing pGK-S1442. We generated pGK-alpha42 as an α-factor peptide-displaying control plasmid, using essentially the same procedure. As other peptide-displaying control plasmids, the gene containing s.s. of α-factor and the mature peptide sequences of angiotensin II (AII) or endothelin-1 (ET1) was inserted into pGK426-tgFLO42 at the NheI and SalI sites, generating pGK-AII42 and pGK-ET142, respectively. As a peptide-non-displaying control plasmid, pGK42 was created in a similar procedure by using the DNA fragment containing s.s. of α-factor without the peptide sequence. pGK-SSTR5-HA [5,6] was used to express human SSTR5 receptor fused to a C-terminal HA tag. Transformation of plasmids was performed using the lithium acetate method. All transformants used for assays are listed in Table S3.

Pheromone Signaling Assay

To assay signal activation from the endogenous Ste2 pheromone receptor, the IMG-4 yeast strains harboring the

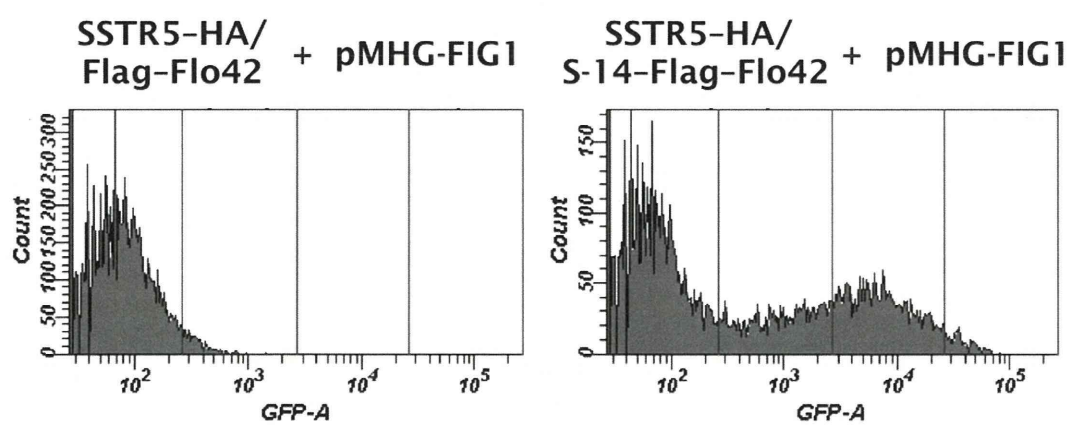

Figure 6. Improved fluorescence signal in the CWTrAP system using somatostatin peptide for the human SSTR5 receptor. SSTR5 signaling assays of the cyclic somatostatin peptide displaying yeast strain and the non-displaying control strain, which contain the multi-copy plasmid harboring a *GFP* reporter gene cassette (pMHG-FIG1). IMFD-70 was used as the host strain. The transformants used in these experiments are listed in Table S3.
doi:10.1371/journal.pone.0037136.g006

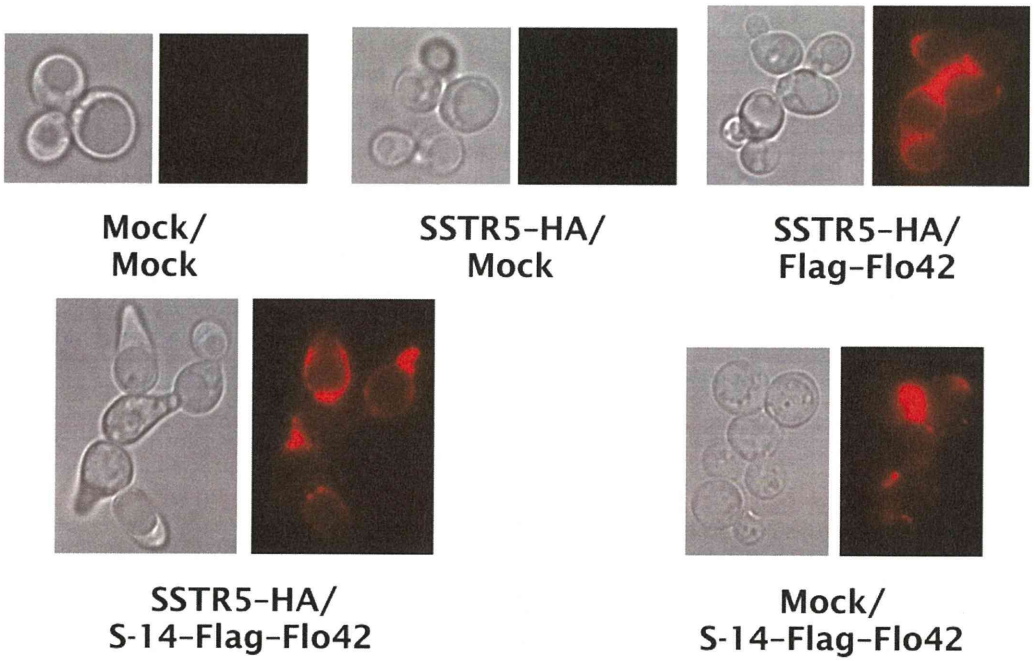

Figure 7. Confirmation of peptide trapping on yeast cell surfaces. Immunofluorescence staining of somatostatin displaying yeast strains. Anti-Flag antibody and Alexa Fluor 594-conjugating secondary antibody were used for detection of Flag–Flo42 anchor or S-14–Flag–Flo42 fusion proteins. Red fluorescence images are shown in false-color. IMFD-70 was used as the host strain. The transformants used in these experiments are listed in Table S3.
doi:10.1371/journal.pone.0037136.g007

pESC-URA-based plasmids were grown in SR media at 30°C, and cells were then inoculated into 100 ml of SRGC media to give an initial optical density of 0.03 at 600 nm. Cultures were grown at 30°C with shaking at 150 opm for 72 h. The cells were collected and diluted into test tubes containing sheath solution and GFP fluorescence was measured using a BD FACSCalibur flow cytometer (BD Biosciences, San Jose, CA, USA). The green fluorescence signal from 10,000 cells was excited with an argon laser and collected through a 530/30 nm band-pass (FL1) filter. The data were analyzed using BD CELLQuest software (BD Biosciences). The "relative fluorescence unit" was defined using the FL1-H geometric mean of IMG-4 harboring mock plasmid (pESC-URA) as the benchmark.

SSTR5 Signaling Assay

To assay signal activation from human SSTR5 receptor, the IMFD-70 yeast strains harboring the pGK-SSTR5-HA and pGK426-based plasmids were grown in SD media at 30°C, and cells were then inoculated into 20 ml of SDM71 media to give an initial OD_{600} of 0.03. Cultures were grown at 30°C with shaking at 150 opm for 15 h. The cells were collected and diluted into test tubes containing sheath solution and GFP fluorescence was measured using a BD FACSCanto II flow cytometer (BD Biosciences). The green fluorescence signal from 10,000 cells was excited with a blue laser and collected through a 530/30 nm band-pass (GFP) filter. The data were analyzed using BD FACSDiva software (BD Biosciences).

Western Blotting

Collected cells were suspended in 10 mM Tris-HCl (pH 7.8) containing 1 mM phenylmethylsulfonyl fluoride (PMSF) to give an OD_{600} of 5, and 200 µl of cell suspension was disrupted using a Multi-beads shocker (Yasui Kikai, Osaka, Japan) with 0.5 mm glass beads. Cell lysates were centrifuged at 1,000×g for 5 min and the pellet was then washed three times with 10 mM Tris-HCl containing 1 mM PMSF. The pellet was resuspended in 200 µl of SDS solubilization buffer (50 mM Tris-HCl [pH 7.8], 2% SDS [w/v], 100 mM ethylene diamine tetraacetic acid [EDTA], 40 mM 2-mercaptoethanol [2-ME]), and the suspension was boiled at 95°C for 5 min and then centrifuged at 10,000×g for 5 min. The supernatant was collected and diluted with an equivalent volume of 2× sample buffer (25 mM Tris-HCl [pH 6.8], 4% SDS [w/v], 20% glycerol [w/v], 10% 2-ME [v/v], 0.1 mg/ml bromophenol blue [BPB]). Twenty microliters of each sample was loaded onto a 12.5% SDS-polyacrylamide gel and proteins were separated by electrophoresis and then transferred to polyvinylidene fluoride (PVDF) membrane (Immobilon-FL; Millipore, Billerica, MA, USA) by electroblotting. Western blots were performed as follows: mouse anti-β-actin monoclonal antibody (Abcam, Cambridge, UK) as loading control, rabbit anti-HA antibody (Bethyl Laboratories, Montgomery, TX, USA) for HA-tagged SSTR5 receptor, and mouse anti-Flag M2 monoclonal antibody (Sigma-Aldrich, St. Louis, MO, USA) for fusion proteins with S-14 peptide, Flag tag and Flo42 anchors were primarily used at dilutions of 1:5,000 in TBST (10 mM Tris-HCl [pH 8.0], 150 mM NaCl, 0.05% Tween-20 [v/v]). Anti-mouse or anti-rabbit secondary antibodies conjugated with alkaline phosphatase (Promega, Madison, WI, USA) were used at dilutions of 1:5,000 in TBST. Chemiluminescent visualization was performed with Amersham CDP-Star Detection Reagent (GE Healthcare, Buckinghamshire, UK) and the signal was detected using a lumino-image analyzer LAS-1000mini system (Fujifilm, Tokyo, Japan).

Immunofluorescent Staining

For α-factor displaying yeasts (IMG-4), collected cells were diluted to give an $OD_{600} = 10$ with distilled water and the cell suspension was used for immunofluorescence staining by incubating with mouse anti-Flag M2 monoclonal antibody (Sigma-Aldrich) at a dilution of 1:500 for 1 h at room temperature. After washing in triplicate, anti-mouse secondary antibody conjugated with Alexa Fluor 546 (Invitrogen Life Technologies, Carlsbad, CA, USA) at a dilution of 1:500 was incubated with the cell suspensions for 1 h at room temperature. After washing in triplicate, cells were resuspended in distilled water and observed on a fluorescence microscope with a monochrome CCD camera. To obtain micrographs of better clarity, essentially the same procedure was used for somatostatin displaying yeasts (IMFD-70), but the density of the collected cells was adjusted to $OD_{600} = 5$. Antibodies were used at a dilution factor of 1:100. Anti-mouse IgG conjugated with Alexa Fluor 594 (Invitrogen Life Technologies) was used as the secondary antibody.

Supporting Information

Figure S1 Western blotting of SDS-extracted fractions from the IMG-4/pUESCαf-FLO42 yeast strain. $EndoH_f$ (Endoglycosidase H) was used to confirm glycosylation of the Flo42 anchor. Anti-Flag M2 monoclonal antibody and anti-mouse secondary antibody conjugated with alkaline phosphatase were used to detect the α-factor Flag Flo42 fusion protein. NBT (nitro blue tetrazolium) and BCIP (5-bromo-4-chloro-3-indolyl-phosphate) were used for the colorimetric reaction.
(TIF)

Figure S2 Pheromone signaling assays of α-factor-displaying yeast strains with various anchor motifs (color histograms). Gray histograms show the data from control strains (mock). IMG-4 was used as the host strain. The transformants used in this experiment are listed in Table S3.
(TIF)

Figure S3 SSTR5 signaling assays of somatostatin-displaying yeast strains with various secretion signal sequences (color histograms). The Flo42 anchor was used for somatostatin display. S-28 indicates the 28 aa active isoform of somatostatin peptide. Gray histograms show the data from control strains (mock). Cultures were grown in SDM71 media for 22 h. IMG-50 was used as the host strain. The transformants used in this experiment are listed in Table S3.
(TIF)

Figure S4 SSTR5 signaling assays of somatostatin-displaying yeast strains with different length GS linkers (color histograms). The S-14 peptide and Flo42 anchor were used for display. Gray histograms show the data from control strains (mock). Cultures were grown in SDM71 media for 12 h. IMG-50 was used as the host strain. The transformants used in this experiment are listed in Table S3.
(TIF)

Figure S5 SSTR5 signaling assays of somatostatin-displaying yeast strain (target cells) mixed with somatostatin-non-displaying strain (non-target cells). S-14–Flag–Flo42 and Flag–Flo42 fusion proteins were used as target and non-target cells, respectively. R1 regions in the dot plots show the gates for FACS sorting. The ratio of initial cell densities was adjusted to 10:1 (non-target cells : target cells), and the cultures were grown in SDM71 media. IMG-50 was used as the host strain. The transformants used in this experiment are listed in Table S3.
(TIF)

Table S1 List of primers.
(PDF)

Table S2 Plasmids used in Supplementary data.
(PDF)

Table S3 List of strains and transformants used for assays.
(PDF)

Document S1 Supplementary Materials and Methods (Plasmid constructions for supporting information).
(PDF)

Acknowledgments

We thank Dr. Ikuo Fujii, Dr. Takeshi Tsumuraya (Osaka Prefecture University), and Dr. Mitsuyoshi Ueda (Kyoto University) for helpful discussion.

Author Contributions

Conceived and designed the experiments: JI NY KT SK CO HF AK. Performed the experiments: JI. Analyzed the data: JI. Contributed reagents/materials/analysis tools: JI. Wrote the paper: JI AK.

References

1. Rasmussen SG, Choi HJ, Rosenbaum DM, Kobilka TS, Thian FS, et al. (2007) Crystal structure of the human β2 adrenergic G-protein-coupled receptor. Nature 450: 383–387.
2. Vögler O, Barceló JM, Ribas C, Escribá PV (2008) Membrane interactions of G proteins and other related proteins. Biochim Biophys Acta 1778: 1640–1652.
3. Ishii J, Fukuda N, Tanaka T, Ogino C, Kondo A (2010) Protein-protein interactions and selection: yeast-based approaches that exploit guanine nucleotide-binding protein signaling. FEBS J 277: 1982–1995.
4. Heilker R, Wolff M, Tautermann CS, Bieler M (2009) G-protein-coupled receptor-focused drug discovery using a target class platform approach. Drug Discov Today 14: 231–240.
5. Togawa S, Ishii J, Ishikura A, Tanaka T, Ogino C, et al. (2010) Importance of asparagine residues at positions 13 and 26 on the amino-terminal domain of human somatostatin receptor subtype-5 in signalling. J Biochem 147: 867–873.
6. Iguchi Y, Ishii J, Nakayama H, Ishikura A, Izawa K, et al. (2010) Control of signalling properties of human somatostatin receptor subtype-5 by additional signal sequences on its amino-terminus in yeast. J Biochem 147: 875–884.
7. Fukuda N, Ishii J, Kaishima M, Kondo A (2011) Amplification of agonist stimulation of human G-protein-coupled receptor signaling in yeast. Anal Biochem 417: 182–187.
8. Ryo S, Ishii J, Iguchi Y, Fukuda N, Kondo A (2012) Transplantation of the GAL regulon into G-protein signaling circuitry in yeast. Anal Biochem 424: 27–31.
9. Li B, Scarselli M, Knudsen CD, Kim SK, Jacobson KA, et al. (2007) Rapid identification of functionally critical amino acids in a G protein-coupled receptor. Nat Methods 4: 169–174.
10. Baranski TJ, Herzmark P, Lichtarge O, Gerber BO, Trueheart J, et al. (1999) C5a receptor activation. Genetic identification of critical residues in four transmembrane helices. J Biol Chem 274: 15757–15765.
11. Ueda M, Tanaka A (2000) Genetic immobilization of proteins on the yeast cell surface. Biotechnol Adv 18: 121–140.
12. Kondo A, Ueda M (2004) Yeast cell-surface display-applications of molecular display. Appl Microbiol Biotechnol 64: 28–40.
13. Shibasaki S, Maeda H, Ueda M (2009) Molecular display technology using yeast-arming technology. Anal Sci 25: 41–49.
14. Gai SA, Wittrup KD (2007) Yeast surface display for protein engineering and characterization. Curr Opin Struct Biol 17: 467–473.
15. Pepper LR, Cho YK, Boder ET, Shusta EV (2008) A decade of yeast surface display technology: where are we now? Comb Chem High Throughput Screen 11: 127–134.
16. Murai T, Ueda M, Atomi H, Shibasaki Y, Kamasawa N, et al. (1997) Genetic immobilization of cellulase on the cell surface of Saccharomyces cerevisiae. Appl Microbiol Biotechnol 48: 499–503.

17. Sato N, Matsumoto T, Ueda M, Tanaka A, Fukuda H, et al. (2002) Long anchor using Flo1 protein enhances reactivity of cell surface-displayed glucoamylase to polymer substrates. Appl Microbiol Biotechnol 60: 469–474.
18. Matsumoto T, Fukuda H, Ueda M, Tanaka A, Kondo A (2002) Construction of yeast strains with high cell surface lipase activity by using novel display systems based on the Flo1p flocculation functional domain. Appl Environ Microbiol 68: 4517–4522.
19. Tanino T, Matsumoto T, Fukuda H, Kondo A (2004) Construction of system for localization of target protein in yeast periplasm using invertase. J Mol Catal, B Enzym 28: 259–264.
20. Nakamura Y, Shibasaki S, Ueda M, Tanaka A, Fukuda H, et al. (2001) Development of novel whole-cell immunoadsorbents by yeast surface display of the IgG-binding domain. Appl Microbiol Biotechnol 57: 500–505.
21. Antipov E, Cho AE, Wittrup KD, Klibanov AM (2008) Highly L and D enantioselective variants of horseradish peroxidase discovered by an ultrahigh-throughput selection method. Proc Natl Acad Sci USA 105: 17694–17699.
22. Feldhaus MJ, Siegel RW, Opresko LK, Coleman JR, Feldhaus JM, et al. (2003) Flow-cytometric isolation of human antibodies from a nonimmune Saccharomyces cerevisiae surface display library. Nat Biotechnol 21: 163–170.
23. Boder ET, Midelfort KS, Wittrup KD (2000) Directed evolution of antibody fragments with monovalent femtomolar antigen-binding affinity. Proc Natl Acad Sci USA 97: 10701–10705.
24. Nakayama N, Miyajima A, Arai K (1987) Common signal transduction system shared by STE2 and STE3 in haploid cells of Saccharomyces cerevisiae: autocrine cell-cycle arrest results from forced expression of STE2. EMBO J 6: 249–254.
25. Dolan JW, Kirkman C, Fields S (1989) The yeast STE12 protein binds to the DNA sequence mediating pheromone induction. Proc Natl Acad Sc. USA 86: 5703–5707.
26. Moller LN, Stidsen CE, Hartmann B, Holst JJ (2003) Somatostatin receptors. Biochim Biophys Acta 1616: 1–84.
27. Burgus R, Ling N, Butcher M, Guillemin R (1973) Primary structure of somatostatin, a hypothalamic peptide that inhibits the secretion of pituitary growth hormone. Proc Natl Acad Sci USA 70: 684–688.
28. Ishii J, Tanaka T, Matsumura S, Tatematsu K, Kuroda S, et al. (2008) Yeast-based fluorescence reporter assay of G protein-coupled receptor signalling for flow cytometric screening: FAR1-disruption recovers loss of episomal plasmid caused by signalling in yeast. J Biochem 143: 667–674.
29. Leberer E, Thomas DY, Whiteway M (1997) Pheromone signalling and polarized morphogenesis in yeast. Curr Opin Genet Dev 7: 59–66.
30. Müller S, Nebe-von-Caron G (2010) Functional single-cell analyses: flow cytometry and cell sorting of microbial populations and communities. FEMS Microbiol Rev 34: 554–587.
31. Brachmann CB, Davies A, Cost GJ, Caputo E, Li J, et al. (1998) Designer deletion strains derived from Saccharomyces cerevisiae S288C: a useful set of strains and plasmids for PCR-mediated gene disruption and other applications. Yeast 14: 115–132.
32. Gietz D, St Jean A, Woods RA, Schiestl RH (1992) Improved method for high efficiency transformation of intact yeast cells. Nucleic Acids Res 20: 1425.
33. MacKay VL, Welch SK, Insley MY, Manney TR, Holly J, et al. (1988) The Saccharomyces cerevisiae BAR1 gene encodes an exported protein with homology to pepsin. Proc Natl Acad Sci USA 85: 55–59.
34. Winzeler EA, Shoemaker DD, Astromoff A, Liang H, Anderson K, et al. (1999) Functional characterization of the S. cerevisiae genome by gene deletion and parallel analysis. Science 285: 901–906.
35. Ishii J, Matsumura S, Kimura S, Tatematsu K, Kuroda S, et al. (2006) Quantitative and dynamic analyses of G protein-coupled receptor signaling in yeast using Fus1, enhanced green fluorescence protein (EGFP), and His3 fusion protein. Biotechnol Prog 22: 954–960.
36. Ishii J, Izawa K, Matsumura S, Wakamura K, Tanino T, et al. (2009) A simple and immediate method for simultaneously evaluating expression level and plasmid maintenance in yeast. J Biochem 145: 701–708.

Analytical Biochemistry 424 (2012) 27–31

Contents lists available at SciVerse ScienceDirect

Analytical Biochemistry

journal homepage: www.elsevier.com/locate/yabio

Transplantation of the GAL regulon into G-protein signaling circuitry in yeast

Shintaro Ryo [a], Jun Ishii [b], Yusuke Iguchi [a], Nobuo Fukuda [a], Akihiko Kondo [a,*]

[a] Department of Chemical Science and Engineering, Graduate School of Engineering, Kobe University, Nada, Kobe 657-8501, Japan
[b] Organization of Advanced Science and Technology, Kobe University, Nada, Kobe 657-8501, Japan

ARTICLE INFO

Article history:
Received 10 December 2011
Accepted 3 February 2012
Available online 13 February 2012

Keywords:
Yeast
G-protein-coupled receptor (GPCR)
Pheromone signaling
GAL regulon
Flow cytometry

ABSTRACT

Here we present a successful transplantation of the GAL genetic regulatory circuitry into the G-protein signaling pathway in yeast. The GAL regulon represents a strictly regulated transcriptional mechanism that we have transplanted into yeast to create a highly robust induction system to assist the detection of on–off switching in G-protein signaling. In our system, we engineered yeast to drive the positive GAL regulatory gene in response to agonist-promoted G-protein signaling and to induce transcription of a green fluorescent protein (*GFP*) reporter gene under the control of the GAL structural gene promoter. Consequently, in response to agonist stimulation of G-protein-coupled receptors (GPCRs), the engineered yeast achieved more than a 150-fold increase in reporter intensity in up to 98% of cells, as determined by flow cytometric sorting. Surprisingly, agonist-stimulated induction of the *GFP* reporter gene was higher than that by galactose. Our approach to boost reporter gene induction could be applicable in establishing more efficient yeast-based flow cytometric screening systems for agonistic ligands for heterogeneous GPCRs.

Transcriptional regulation in eukaryotes often requires the cooperation of many proteins to bind to the upstream region of a gene [1]. Such highly regulated transcriptional networks frequently possess negative feedback or positive feedback loops capable of suppressing transcriptional noise or amplifying transcription [1,2].

The GAL regulatory network in *Saccharomyces cerevisiae* is one of the most studied genetic networks [3]. The structural genes (*GAL2*, *GAL1*, *GAL7*, and *GAL10*) of the GAL network operate to regulate galactose transport and metabolism [1,2], with their expression regulated by the presence of glucose and galactose [4]. The regulatory genes (*GAL4*, *GAL80*, and *GAL3*) involve a mechanism for swift transcriptional activation of the GAL genes in the presence of galactose [5]. The transcriptional activator Gal4 binds to the upstream activation sequence (UAS_{GAL})[1] and transcribes the GAL genes, whereas Gal80 and Gal3 provide negative and positive feedback on GAL expression, respectively [2,3]. In the absence of galactose, Gal80 interacts with Gal4 to inhibit its activity, whereas the galactose-bound Gal3 interacts with Gal80 to relieve the inhibition of Gal4 and permit the expression of the GAL genes [5] (Fig. 1A). Because the GAL genetic circuitry is well characterized and strictly regulated, the promoters of GAL genes such as *GAL1*, which induces intensive transcriptional activation, are often used as a highly robust induction system. Yeast contains guanine nucleotide-binding proteins (G-proteins) and G-protein-coupled receptors (GPCRs) as peripheral membrane and trans-membrane proteins. In humans, GPCRs are involved in the control of many physiological functions such as taste, smell, vision, heart rate, blood pressure, neurotransmission, and cell growth [6]; therefore, they are considered as attractive pharmaceutical and therapeutic targets [7]. The eukaryotic unicellular *S. cerevisiae* is a familiar host cell system to study GPCR signaling because its uncompetitive and monopolistic G-protein signaling pathway (pheromone signaling pathway) can simplify the analyses of complicated mammalian GPCR signaling systems [8–12]. The existence of signal-responsive assay systems using transcriptional reporter genes such as *HIS3* (auxotrophy), *lacZ* (colorimetry), and *luc* (luminometry) means that yeast is an easy-to-use analytical tool [12–15]. In general, because high sensitivity is a requirement of most assays, reporter sensitivity is an important determinant when considering an experimental approach.

Here, we report the successful transplantation of the GAL genetic regulatory circuitry into the G-protein signaling pathway in yeast. We were able to engineer transcriptional activation of the GAL regulon downstream of GPCR activation (Fig. 1B–D) in order to produce a robust and inducible expression system capable of significant reporter expression even in the absence of galactose. In the current study, the endogenous yeast GPCR (Ste2) and its natural ligand (α-factor) were used to demonstrate our concept. In addition, we used a green fluorescent protein (*GFP*) reporter gene with the future aim of applying this system to quantitative, high-throughput screening using flow cytometry.

* Corresponding author. Fax: +81 78 803 6196.
E-mail address: akondo@kobe-u.ac.jp (A. Kondo).

[1] *Abbreviations used:* UAS, upstream activation sequence; G-protein, guanine nucleotide-binding protein; GPCR, G-protein-coupled receptor; YNB, yeast nitrogen base without amino acids; GFP, green fluorescent protein; EGFP, enhanced green fluorescent protein; PCR, polymerase chain reaction; $Gal3^c$, constitutively active Gal3 mutant; EC_{50}, half-maximal effective concentration.

0003-2697/$ - see front matter © 2012 Elsevier Inc. All rights reserved.
doi:10.1016/j.ab.2012.02.005

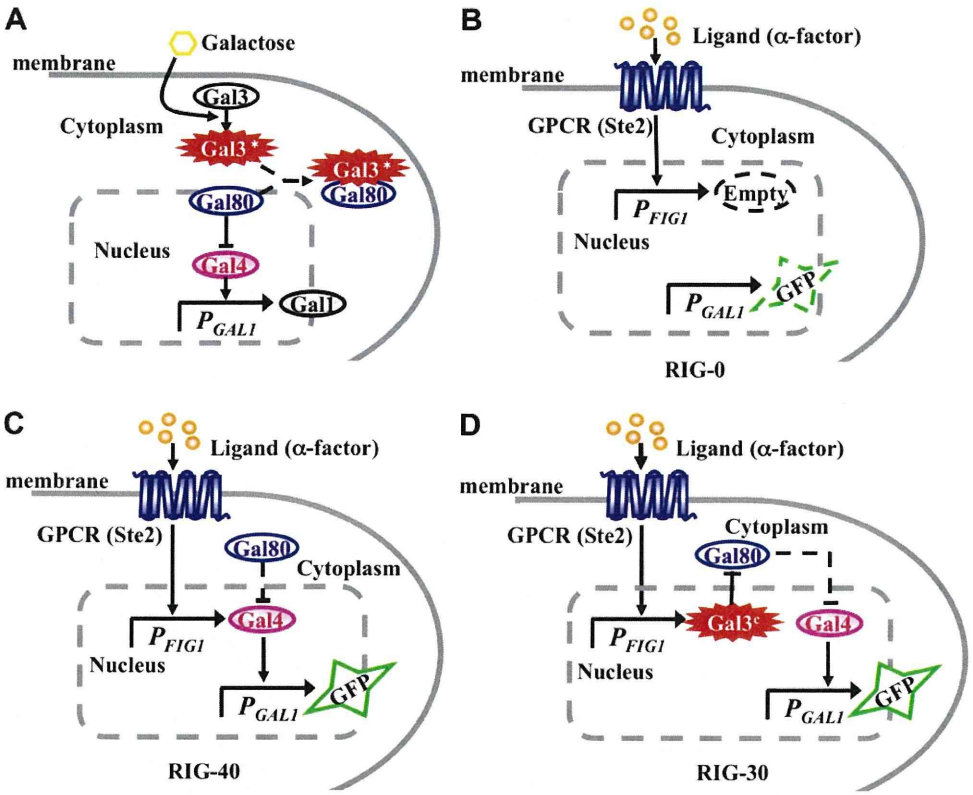

Fig.1. Outline of the experimental design. (A) GAL genetic regulatory network in wild-type yeast. The transcription of GAL structural genes (including *GAL1*) is strictly regulated by the GAL regulatory genes (*GAL4*, *GAL80*, and *GAL3*). Without galactose (in the presence of glucose), Gal80 binds to the transcriptional activator Gal4 and inhibits expression of *GAL1*. In the presence of galactose, the galactose-bound Gal3 (Gal3*) interacts with Gal80 and relieves the inhibition of Gal4, permitting the expression of *GAL1*. (B–D) Transplantation of GAL genetic regulatory circuitry into G-protein signaling pathway in yeast. (B) The RIG-0 control strain is engineered to express the *GFP* reporter gene under the control of the *GAL1* promoter. The RIG-0 control strain was used for construction of the RIG-40 and RIG-30 yeast strains. (C) The RIG-40 strain is engineered to express the transcriptional activator *GAL4* gene in response to an agonist-promoted signal from a GPCR. Signal-dependent Gal4 expression could induce *GFP* transcription due to a lack of inhibition of Gal80 (Gal4 repressor). (D) The RIG-30 strain is engineered to express a constitutively active mutant of Gal3 ($Gal3^c$) in response to an agonist-promoted signal from a GPCR. Signal-dependent expression of $Gal3^c$ then binds to Gal80, inhibiting its activity and inducing *GFP* transcription.

Materials and methods

Media

YPD medium contained 1% yeast extract (Nacalai Tesque, Kyoto, Japan), 2% peptone (BD Diagnostic Systems, Sparks, MD, USA), and 2% glucose. SD medium contained 0.67% yeast nitrogen base without amino acids (YNB) (BD Diagnostic Systems) and 2% glucose. SG medium contained 0.67% YNB and 2% galactose. SDLG medium contained 0.67% YNB, 3% glycerol, 0.05% glucose, and 2% lithium lactate (Sigma–Aldrich, St. Louis, MO, USA) [16]. Amino acids and nucleotides (20 mg/L histidine, 60 mg/L leucine, 20 mg/L methionine, and 20 mg/L uracil) were supplemented into each medium to lack the relevant auxotrophic components. For SDLG medium, amino acids complete drop-out mix was additionally supplemented to lack the relevant auxotrophic components.

Plasmid construction

All plasmids used in this study are summarized in Table 1. All primers used for the plasmid constructions are listed in Supplementary Table 1 in the supplementary material. The amplified DNA fragments encoding the *GAL1* promoter (600 bp) and the enhanced green fluorescent protein (*EGFP*) were digested with *Bam*HI and *Xba*I and with *Xba*I and *Sal*I, respectively, and were simultaneously inserted at *Bam*HI and *Sal*I sites into pUC19 vector (Takara Bio, Shiga, Japan), resulting in pUC19-12. The DNA fragments encoding the *URA3* selectable marker (with 50 nucleotides from the 5′ side of the *GAL1* terminator at the 5′ end) and the *GAL1* terminator (800 bp) were amplified by overlap polymerase chain reaction (PCR), and the conjugated fragment was inserted at *Sph*I and *Sal*I sites into pUC19-12, creating pGAL1pt–EGFP. The amplified DNA fragment encoding the *GAL3* gene was inserted at *Bam*HI and *Sac*II sites into pBlueScript II KS(+) vector (Agilent Technologies, Santa Clara, CA, USA), generating pBlue–GAL3. To introduce the S509P point mutation into the *GAL3* gene [16], QuikChange site-directed mutagenesis (Agilent Technologies) was carried out using pBlue–GAL3 as a template according to the manufacturer's protocol, creating pBlue–$GAL3^c$. The amplified DNA fragment corresponding to the *FIG1* promoter (600 bp) was inserted at *Eco*RI and *Sac*I sites into pUC19 vector, resulting in pUC19–FIG1p. The amplified DNA fragment containing the *URA3* selectable marker (with 40 nucleotides from the 5′ side of the *FIG1* terminator at the 5′ end) and the *FIG1* terminator (300 bp) from pFIG450GF [11] was inserted at *Sma*I and *Hin*dIII sites into pUC19–FIG1p, making pUC19–FIG1ptURA3. The amplified DNA fragment encoding the *GAL4* gene was inserted at *Sac*I and *Sma*I sites into pUC19–FIG1ptURA3, producing pFIG1pt–GAL4. The digested DNA fragment encoding the $GAL3^c$ gene was prepared from pBlue–$GAL3^c$ and inserted at *Sac*I and *Sma*I sites into pUC19–FIG1ptURA3, producing pFIG1pt–$GAL3^c$.

Yeast strain construction

Yeast strains used in this study are listed in Table 1. We used the lithium acetate method to transform these strains with linear

Table 1
Yeast strains and plasmids.

Strain or plasmid	Description	Reference
Strain		
BY4741	*MATa his*Δ*1 leu2*Δ*0 met15*Δ*0 ura3*Δ*0*	[19]
MI-7	BY4741 *sst2*Δ*::kanMX4 far1*Δ	This study
RIG-0	MI-7 *gal1*Δ*::EGFP*	This study
RIG-30	RIG-0 *fig1*Δ*::GAL3^c*	This study
RIG-40	RIG-0 *fig1*Δ*::GAL4*	This study
Plasmid		
pUC19	Cloning vector	Takara Bio
pUC19-12	P_{GAL1}*(600 bp)–EGFP* in pUC19	This study
pGAL1pt-EGFP	P_{GAL1}*(600 bp)–EGFP–*T_{GAL1}*(50 bp)-URA3–*T_{GAL1}*(800 bp)* in pUC19	This study
pBlueScript II KS(+)	Cloning vector	Agilent Technologies
pBlue-GAL3	*GAL3* in pBlueScript II KS(+)	This study
pBlue-GAL3^c	*GAL3^c* (S509P point mutation in Gal3) in pBlueScript II KS(+)	This study
pUC19-FIG1p	P_{FIG1}*(600 bp)* in pUC19	This study
pFIG450GF	P_{FIG1}*(450 bp)–EGFP–*T_{FIG1}*(40 bp)–URA3–*T_{FIG1}*(300 bp)* in pUC119	[11]
pUC19-FIG1ptURA3	P_{FIG1}*(600 bp)–*T_{FIG1}*(40 bp)–URA3–*T_{FIG1}*(300 bp)* in pUC19	This study
pFIG1pt-GAL4	P_{FIG1}*(600 bp)–GAL4–*T_{FIG1}*(40 bp)–URA3–*T_{FIG1}*(300 bp)* in pUC19	This study
pFIG1pt-GAL3^c	P_{FIG1}*(600 bp)–GAL3^c–*T_{FIG1}*(40 bp)–URA3–*T_{FIG1}*(300 bp)* in pUC19	This study

DNA fragments [17]. All homologous recombination procedures followed the marker recycle method [18] to eliminate and reuse the *URA3* selectable marker. To generate the MI-7 yeast strain, the *far1*Δ allele was inserted into an *sst2*Δ single mutant strain derived from BY4741 [19] (obtained from the *Saccharomyces* Genome Deletion Project [20]), essentially as described previously [10]. To construct the recombinant yeast strain in which the genomic *GAL1* gene was replaced by the *EGFP* reporter gene, the DNA fragment obtained by digesting pGAL1pt–EGFP with *Bgl*I and *Bgl*II was introduced into MI-7. We designated the *URA3*-eliminated strain as RIG-0. To produce the recombinant yeast strain in which the genomic *FIG1* gene was replaced by the *GAL4* gene, the DNA fragment obtained by digesting pFIG1pt–GAL4 with *Ahd*I and *Hin*dIII was introduced into RIG-0. We designated the *URA3*-eliminated strain as RIG-40. Similarly, to fabricate the recombinant yeast strain in which the genomic *FIG1* gene was replaced by the *GAL3^c* gene, the DNA fragment obtained by digesting pFIG1pt–GAL3^c with *Ahd*I and *Hin*dIII was introduced into RIG-0. We designated the *URA3*-eliminated strain as RIG-30.

Pheromone signaling assay

Recombinant yeast strains (RIG-0, RIG-30, and RIG-40) precultivated in YPD medium for 12 h were inoculated into 3 ml of SDLG medium containing indicated concentrations of α-factor (Zymo Research, Orange, CA, USA) to give an initial optical density of 0.1 at 600 nm. They were grown at 30 °C with shaking at 150 rpm for 18 h. Then, the cells were suspended into 1 ml of sheath solution, and GFP fluorescence was analyzed by a BD FACSCanto II flow cytometer equipped with a 488-nm blue laser (BD Biosciences, San Jose, CA, USA). The GFP fluorescence signal was collected through a 530/30-nm bandpass filter, and the mean of fluorescence intensity was defined as the GFP-A mean of 10,000 cells. The data were analyzed using BD FACSDiva software (version 5.0, BD Biosciences) and FlowJo software (version 8.5.3, Tree Star, Ashland, OR, USA).

Galactose-mediated induction of GAL regulon

RIG-0 yeast strain was grown in SD or SG medium without α-factor to check the induction level of the *GAL1* promoter by galactose. GFP fluorescence was measured as for the pheromone signaling assay.

Results and discussion

The aim of this study was to incorporate the GAL genetic regulatory circuitry into the G-protein signaling pathway in the yeast *S. cerevisiae* in order to establish a highly robust reporter gene assay system for detecting on–off switching in G-protein signaling, responding to agonist stimulation of GPCRs. To achieve this, we designed recombinant yeast strains to induce transcription of the genetically introduced GAL regulon in response to activation of the G-protein (pheromone) signaling pathway. As a specific strategy, yeast was engineered to express Gal4 or a constitutively active Gal3 mutant (Gal3^c) [16] under the control of the pheromone-responsive *FIG1* promoter, a commonly used reporter gene to detect G-protein signaling [10,11] (Fig. 1B–D). The overexpression of Gal4 was expected to directly activate the transcription of GAL genes (Fig. 1C), whereas the induction of Gal3^c was expected to promote transcription of GAL genes through the activation of Gal4 protein (Fig. 1D). We used the *GAL1* promoter, as the output of agonist stimulation, to induce expression of the *GFP* reporter gene (Fig. 1B–D).

First, we constructed the MI-7 yeast strain harboring *sst2*Δ and *far1*Δ double deletion alleles that confer advantages in GPCR signaling assays by increasing sensitivity to the agonistic ligand and inhibiting cell cycle arrest [21]. Using MI-7 as a backbone strain, we replaced the genomic *GAL1* gene with the *GFP* reporter gene, generating the RIG-0 yeast strain (Table 1). To check the induction

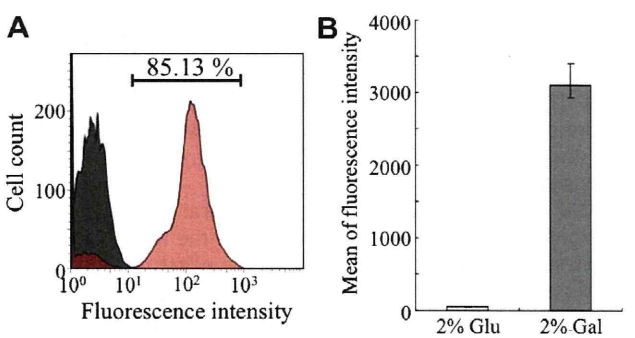

Fig.2. Induction of *GFP* reporter gene in the presence of galactose. To check induction of the *GFP* reporter gene by the *GAL1* promoter in the presence of galactose, the RIG-0 yeast strain, whose *GAL1* gene was replaced by the *GFP* gene, was incubated in SD medium (containing 2% glucose) or SG medium (containing 2% galactose) for 18 h. The GFP fluorescence of 10,000 cells was measured by flow cytometry. (A) Histogram plots of RIG-0 strain grown in SD medium (filled gray) and in SG medium (filled red). (B) Mean values of the green fluorescence signal of 10,000 cells. Error bars represent the standard deviations ($n = 3$). (For interpretation of the references to color in this figure legend, the reader is referred to the Web version of this article.)

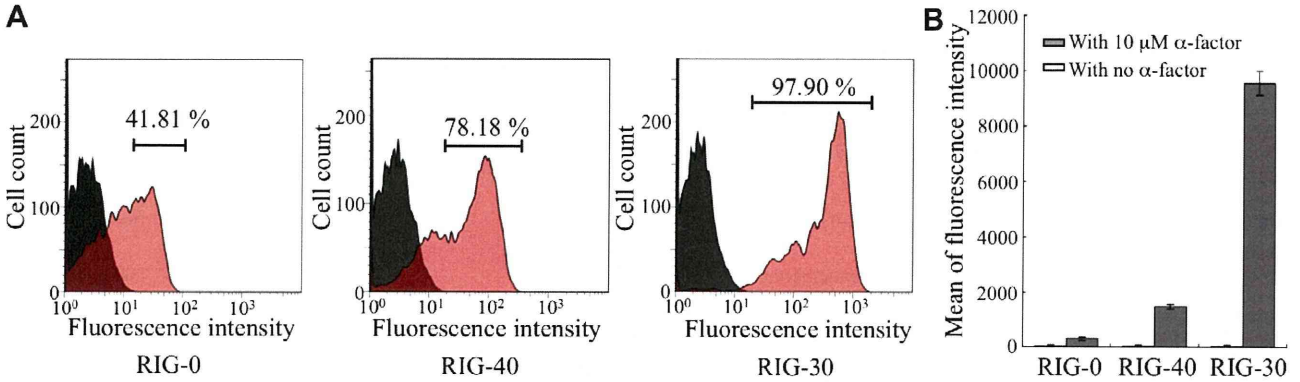

Fig.3. Effect of agonist-induced GPCR signaling on induction of the *GFP* reporter gene in GAL regulon transplanted yeast strains. The RIG-0 strain, whose *GAL1* gene was replaced by the *GFP* gene, was used as a control strain. Based on the RIG-0 strain, we generated the RIG-40 and RIG-30 strains that express the *GAL4* and *GAL3*^{c} genes, respectively, under the control of the pheromone-responsive *FIG1* promoter. All engineered strains were incubated in SDLG medium with or without 10 μM α-factor for 18 h. The GFP fluorescence of 10,000 cells was measured by a flow cytometer. (A) Histogram plots of RIG-0, RIG-40, and RIG-30 strains grown without α-factor (filled gray) and with 10 μM α-factor (filled red). (B) Mean values of the green fluorescence signal of 10,000 cells. Error bars represent the standard deviations (n = 3). (For interpretation of the references to color in this figure legend, the reader is referred to the Web version of this article.)

level of the *GFP* reporter gene by the *GAL1* promoter in the presence of galactose, the RIG-0 strain was cultivated in medium containing 2% glucose (without induction) or 2% galactose (with induction) as a carbon source. We then measured the GFP fluorescence level of each yeast cell by flow cytometry (Fig. 2A). As expected, the average fluorescence of RIG-0 was elevated in the presence of galactose, exhibiting a greater than 50-fold increase in fluorescence intensity compared with cultivation in the presence of glucose (Fig. 2B). Thus, in the RIG-0 strain, the galactose-mediated GAL regulatory machinery was able to induce the *GFP* reporter gene robustly under the control of the *GAL1* promoter.

To verify the validity of our concept, the *GAL4* or *GAL3*^{c} gene was substituted for the pheromone-responsive *FIG1* gene in the genome of RIG-0, yielding the RIG-40 or RIG-30 strain, respectively (Table 1). For activation of G-protein signaling, the engineered yeast strains were cultivated in galactose-free glycerol/lactate medium (containing marginal glucose of 0.05%) with or without 10 μM α-factor, and the fluorescence level of each yeast cell was measured by flow cytometry (Fig. 3). As expected, the introduction of the *GAL4* or *GAL3*^{c} gene into the pheromone-responsive gene locus of the RIG-0 strain induced GFP fluorescence downstream of GPCR stimulation (Fig. 3A). Surprisingly, the induction level of the *GFP* reporter gene in response to GPCR stimulation was higher than that by galactose (Fig. 2). The limited fluorescence of the RIG-0 negative control strain in the presence of α-factor probably reflected changes in intrinsic fluorescence invoked by signal activation (Fig. 3A). Whereas agonist stimulation increased GFP fluorescence in the RIG-40 strain approximately 25-fold, the RIG-30 displayed a greater than 150-fold increase in fluorescence intensity (Fig. 3B).

One possible explanation for this critical difference between pheromone-responsive GFP expression of the RIG-40 and RIG-30 yeast strains may be due largely to the effect of Gal80 (a Gal4 repressor), which promotes Gal4-mediated transcription by interacting with Gal3^{c}. Indeed, we observed that a yeast strain that lacks Gal80 (*gal80Δ*), with an integrated *GFP* reporter gene in the *GAL1* locus, produced a green fluorescent signal even in the absence of α-factor stimulation (data not shown). Briefly, Gal80 not bound to endogenous Gal4 might inhibit the activity of pheromone-induced overexpressed Gal4 because Gal4 is the direct transcriptional activator of the GAL regulon. However, the constitutively active Gal3 mutant, Gal3^{c}, is capable of activating the GAL regulon because it can inhibit the Gal80/Gal4 interaction despite the presence of endogenous Gal80 [22–25].

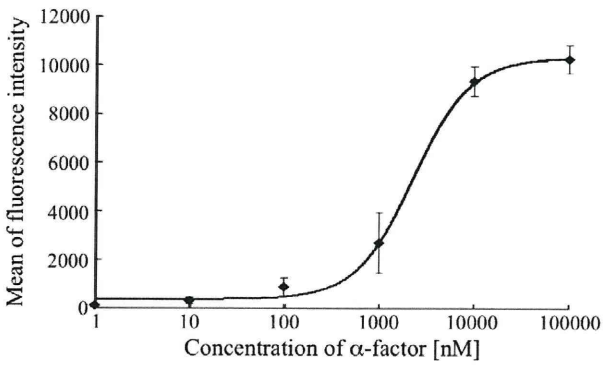

Fig.4. Dose–response curve for various concentrations of α-factor in GAL regulon engineered RIG-30 strain. The RIG-30 strain, whose *GAL1* gene and *FIG1* gene were replaced by the *GFP* and *GAL3*^{c} genes, respectively, was incubated in SDLG medium with indicated concentrations of α-factor for 18 h. The GFP fluorescence of 10,000 cells was measured by a flow cytometer. Mean values of the green fluorescence signal of 10,000 cells are shown. Error bars represent the standard deviations (n = 3).

In addition, we examined the data from our engineered yeast strains to test the assumption that our system could be applied for the screening of novel GPCR agonists by flow cytometry Ishii et al. [26] (Fig. 3A). Flow cytometry easily distinguished the agonist-stimulated RIG-30 yeast cells from the nonactivated cells, with a significant GFP signal detected in up to 98% of the cell population, supporting the possibility that our method could easily permit quantitative, high-throughput, flow cytometric screening of novel GPCR agonists.

Finally, we investigated whether we could use our system as a sensing tool for agonist-specific signaling. As shown in Fig. 4, the RIG-30 exhibited a dose-dependent increase in GFP fluorescence, the result of increasing α-factor concentration. Moreover, the half-maximal effective concentration (EC_{50}) was calculated to be 1.43 ± 0.27 μM. These results clearly show a significant and sensitive GFP reporter induction in RIG-30, the result of the GPCR ligand α-factor.

Conclusion

In this study, we successfully established a highly robust reporter gene assay system for detecting GPCR agonists by transplanting the GAL regulon into G-protein signaling circuitry in yeast. Our

system, designed to express the constitutively active Gal3 mutant ($Gal3^c$) under the control of the pheromone-responsive *FIG1* promoter, agonist stimulation achieved a greater than 150-fold increase in reporter intensity. In addition, flow cytometry screening could distinguish an agonist-induced signal in up to 98% of cells. Our method could be applied to the quantitative, high-throughput screening of novel GPCR agonists.

Acknowledgments

This work was supported by Special Coordination Funds for Promoting Science and Technology, Creation of Innovation Centers for Advanced Interdisciplinary Research Areas (Innovative Bioproduction Kobe, iBioK), MEXT, Japan, and funded in part by the Naito Foundation.

Appendix A. Supplementary data

Supplementary data associated with this article can be found, in the online version, at doi:10.1016/j.ab.2012.02.005.

References

[1] A. Traven, B. Jelicic, M. Sopta, Yeast Gal4: a transcriptional paradigm revisited, EMBO Rep. 7 (2006) 496–499.
[2] S.A. Ramsey, J.J. Smith, D. Orrell, M. Marelli, T.W. Petersen, P. de Atauri, H. Bolouri, J.D. Aitchison, Dual feedback loops in the GAL regulon suppress cellular heterogeneity in yeast, Nat. Genet. 38 (2006) 10082–10087.
[3] R. Yang, S.C. Lenaghan, J.P. Wikswo, M. Zhang, External control of the GAL network in *S. cerevisiae*: a view from control theory, PLoS One 6 (2011) 19353.
[4] O. Demir, I. Aksan Kurnaz, An integrated model of glucose and galactose metabolism regulated by the GAL genetic switch, Biol. Chem. 30 (2006) 179–192.
[5] C.Q. Diep, X. Tao, V. Pilauri, M. Losiewicz, T.E. Blank, J.E. Hopper, Genetic evidence for sites of interaction between the Gal3 and Gal80 proteins of the *Saccharomyces cerevisiae* GAL gene switch, Genetics 178 (2008) 725–736.
[6] J. Ishii, N. Fukuda, T. Tanaka, C. Ogino, A. Kondo, Protein–protein interactions and selection: yeast-based approaches that exploit guanine nucleotide-binding protein signaling, FEBS J. 277 (2010) 1982–1995.
[7] R. Heilker, M. Wolff, C.S. Tautermann, M. Bieler, G-protein-coupled receptor-focused drug discovery using a target class platform approach, Drug Discov. Today 14 (2009) 231–240.
[8] G.D. Stewart, C. Valant, S.J. Dowell, D. Mijaljica, R.J. Devenish, P.J. Scammells, P.M. Sexton, A. Christopoulos, Determination of adenosine A1 receptor agonist and antagonist pharmacology using *Saccharomyces cerevisiae*: implications for ligand screening and functional selectivity, J. Pharmacol. Exp. Ther. 331 (2009) 277–286.
[9] S.J. Dowell, A.J. Brown, Yeast assays for G-protein-coupled receptors, Receptors Channels 8 (2002) 343–352.
[10] Y. Iguchi, J. Ishii, H. Nakayama, A. Ishikura, K. Izawa, T. Tanaka, C. Ogino, A. Kondo, Control of signalling properties of human somatostatin receptor subtype-5 by additional signal sequences on its amino-terminus in yeast, J. Biochem. 147 (2010) 875–884.
[11] S. Togawa, J. Ishii, A. Ishikura, T. Tanaka, C. Ogino, A. Kondo, Importance of asparagine residues at positions 13 and 26 on the amino-terminal domain of human somatostatin receptor subtype-5 in signaling, J. Biochem. 147 (2010) 867–873.
[12] Y. Fukutani, T. Nakamura, M. Yorozu, J. Ishii, A. Kondo, M. Yohda, The N-terminal replacement of an olfactory receptor for the development of a yeast-based biomimetic odor sensor, Biotechnol. Bioeng. 109 (2012) 205–212.
[13] B.J. Evans, Z. Wang, J.R. Broach, S. Oishi, N. Fujii, S.C. Peiper, Expression of CXCR4, a G-protein-coupled receptor for CXCL12 in yeast identification of new-generation inverse agonists, Methods Enzymol. 460 (2009) 399–412.
[14] G. Ladds, A. Goddard, J. Davey, Functional analysis of heterologous GPCR signalling pathways in yeast, Trends Biotechnol. 23 (2005) 367–373.
[15] R. Panetta, Y. Guo, S. Magder, M.T. Greenwood, Regulators of G-protein signaling (RGS) 1 and 16 are induced in response to bacterial lipopolysaccharide and stimulate c-fos promoter expression, Biochem. Biophys. Res. Commun. 259 (1999) 550–556.
[16] C.Q. Diep, G. Peng, M. Bewley, V. Pilauri, I. Ropson, J.E. Hopper, Intragenic suppression of Gal3C interaction with Gal80 in the *Saccharomyces cerevisiae* GAL gene switch, Genetics 172 (2006) 77–87.
[17] D. Gietz, A. St. Jean, R.A. Woods, R.H. Schiestl, Improved method for high efficiency transformation of intact yeast cells, Nucleic Acids Res. 20 (1992) 1425.
[18] R. Akada, T. Kitagawa, S. Kaneko, D. Toyonaga, S. Ito, Y. Kakihara, H. Hoshida, S. Morimura, A. Kondo, K. Kida, PCR-mediated seamless gene deletion and marker recycling in *Saccharomyces cerevisiae*, Yeast 23 (2006) 399–405.
[19] C.B. Brachmann, A. Davies, G.J. Cost, E. Caputo, J. Li, P. Hieter, J.D. Boeke, Designer deletion strains derived from *Saccharomyces cerevisiae* S288C: a useful set of strains and plasmids for PCR-mediated gene disruption and other applications, Yeast 14 (1998) 115–132.
[20] E.A. Winzeler, D.D. Shoemaker, A. Astromoff, H. Liang, K. Anderson, B. Andre, R. Bangham, R. Benito, J.D. Boeke, H. Bussey, A.M. Chu, C. Connelly, K. Davis, F. Dietrich, S.W. Dow, M. El Bakkoury, F. Foury, S.H. Friend, E. Gentalen, G. Giaever, J.H. Hegemann, T. Jones, M. Laub, H. Liao, N. Liebundguth, D.J. Lockhart, A. Lucau-Danila, M. Lussier, N. M'Rabet, P. Menard, M. Mittmann, C. Pai, C. Rebischung, J.L. Revuelta, L. Riles, C.J. Roberts, P. Ross-MacDonald, B. Scherens, M. Snyder, S. Sookhai-Mahadeo, R.K. Storms, S. Véronneau, M. Voet, G. Volckaert, T.R. Ward, R. Wysocki, G.S. Yen, K. Yu, K. Zimmermann, P. Philippsen, M. Johnston, R.W. Davis, Functional characterization of the *S. cerevisiae* genome by gene deletion and parallel analysis, Science 285 (1995) 901–906.
[21] J. Ishii, T. Tanaka, S. Matsumura, K. Tatematsu, S. Kuroda, C. Ogino, H. Fukuda, A. Kondo, Yeast-based fluorescence reporter assay of G protein-coupled receptor signalling for flow cytometric screening: FAR1-disruption recovers loss of episomal plasmid caused by signalling in yeast, J. Biochem. 143 (2008) 667–674.
[22] M. Rubio-Texeira, A comparative analysis of the GAL genetic switch between not-so-distant cousins *Saccharomyces cerevisiae* versus *Kluyveromyces lactis*, FEMS Yeast Res. 5 (2005) 1115–1128.
[23] P.J. Bhat, T.V. Murthy, Transcriptional control of the GAL/MEL regulon of yeast *Saccharomyces cerevisiae:* mechanism of galactose-mediated signal transduction, Mol. Microbiol. 40 (2001) 1059–1066.
[24] O. Egriboz, F. Jiang, J.E. Hopper, The rapid GAL gene switch of *Saccharomyces cerevisiae* depends on nuclear Gal3, not nucleo-cytoplasmic trafficking of Gal3 and Gal80, Genetics 189 (2011) 825–836.
[25] R. Wightman, R. Bell, R.J. Reece, Localization and interaction of the proteins constituting the GAL genetic switch in *Saccharomyces cerevisiae*, Eukaryot. Cell 7 (2008) 2061–2068.
[26] J. Ishii, N. Yoshimoto, K. Tatematsu, S. Kuroda, C. Ogino, H. Fukuda, A. Kondo, Cell wall trapping of autocrine peptides for human G-protein-coupled receptors on the yeast cell surface, PLoS ONE, submitted for publication.

Bioorganic & Medicinal Chemistry 20 (2012) 16–24

Contents lists available at SciVerse ScienceDirect

Bioorganic & Medicinal Chemistry

journal homepage: www.elsevier.com/locate/bmc

Nucleic acid probe containing fluorescent tricyclic base-linked acyclonucleoside for detection of single nucleotide polymorphisms

Kinji Furukawa [a,†], Mayumi Hattori [a,†], Tokimitsu Ohki [a], Yoshiaki Kitamura [a], Yukio Kitade [a], Yoshihito Ueno [b,*]

[a] Department of Biomolecular Science, Faculty of Engineering, Gifu University, 1-1 Yanagido, Gifu 501-1193, Japan
[b] Department of Applied Life Science, Faculty of Applied Biological Sciences, Gifu University, 1-1 Yanagido, Gifu 501-1193, Japan

ARTICLE INFO

Article history:
Received 22 October 2011
Revised 19 November 2011
Accepted 21 November 2011
Available online 1 December 2011

Keywords:
DNA
SNPs
Detection
Acyclonucleoside
Tricyclic base

ABSTRACT

The development of a reliable and simple method for detecting single nucleotide polymorphisms (SNPs), common genetic variations in the human genome, is currently an important research area because SNPs are important for identifying disease-causing genes and for pharmacogenetic studies. Here, we developed a novel method for SNP detection. We designed and synthesized DNA probes containing a fluorescent tricyclic base-linked acyclonucleoside **P**. The type of nucleobases involved in the SNP sites in the DNA and RNA targets could be determined using four DNA probes containing **P**. Thus, this system would provide a novel and simple method for detecting SNPs in DNA and RNA targets.

1. Introduction

The most frequent form of genetic variation in the human genome is a single nucleotide polymorphism (SNP), which occurs roughly once every 1000 bases and is currently thought to be linked to diseases and individual differences in drug response.[1,2] Therefore, the development of a reliable and simple method for detecting SNPs is very important for pharmacogenomics[3] and the realization of personalized medicine. To date, a number of SNP genotyping technologies, such as microarrays,[4,5] molecular inversion probe genotyping,[6] 5′ exonuclease fluorescence-based assay (Taq-Man),[7] pyrosequencing,[8] single-base extension[9] and matrix-assisted laser desorption/ionization time-of-flight mass spectrometry (MALDI-TOF/MS),[10,11] have been developed and applied. Most discrimination principles in these methods are based on differences in the thermodynamic stabilities of the duplexes comprising a probe strand and a complementary DNA target or DNA containing SNPs; the probe binds to the wild-type sequence but not to DNA containing SNPs. However, because differences in duplex stabilities between complementary sequences and sequences containing one base mismatch are small, careful selection of the oligonucleotide probe sequence and the annealing conditions, especially temperature, is needed to prevent genotyping errors.

It would be advantageous to directly detect the formation of base pairing with a target nucleoside, for example, hydrogen bonding with a target nucleobase, as a fluorescence signal in duplex formation. Saito and colleagues reported that oligodeoxynucleotides (ODNs) containing base-discriminating fluorescent (BDF) nucleosides that were modified with a pyrene or dimethylaminonaphthalene residue acted as nucleic acid probes.[12–17] Seitz and colleagues also reported forced intercalation probes (FIT-probes), which contained thiazole orange as a fluorescent base.[18–22]

In this paper, we report a novel method for SNP detection using a nucleic acid probe that contains a fluorescent tricyclic base-linked acyclonucleoside, 8-amino-3-(2,3-dihydroxypropyl) imidazo[4′,5′:5,6]pyrido[2,3-*d*]pyrimidine (**P**) (Fig. 1). The design principle of SNP detection using the nucleoside surrogate **P** is outlined in Figure 2. The fluorescence intensity of the tricyclic base-linked **P** depended on solvent polarity; fluorescence intensity

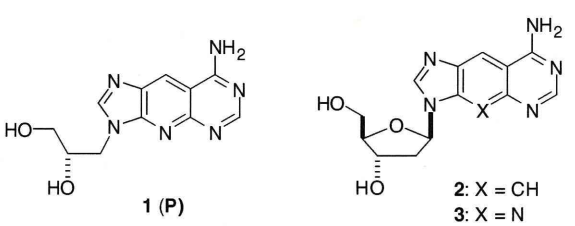

Figure 1. Structures of tricyclic base-linked nucleoside surrogates.

* Corresponding authors. Tel./fax: +81 58 293 2919.
E-mail address: uenoy@gifu-u.ac.jp (Y. Ueno).
† These authors contributed equally to this work.

0968-0896/$ - see front matter © 2011 Elsevier Ltd. All rights reserved.
doi:10.1016/j.bmc.2011.11.045

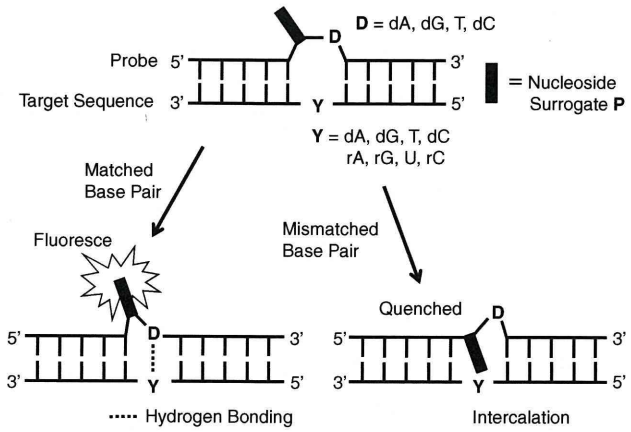

Figure 2. Design principle of SNP detection using the nucleoside surrogate **P**. **D**s denotes discriminating bases. **Y**s indicates SNP sites.

of **P** was greater in more polar solvents such as methanol and water compared to less polar solvents such as chloroform. Based on this result, we designed nucleic acid probes containing **P** at the 5′ (5′-P-probes) or 3′ sides (3′-P-probes) of discriminating bases **D**s to produce bulges. It is believed that the inside of the grooves of the DNA helix is more hydrophobic than bulk water.[23] Thus, we presumed that when the **D**s match the sequences of opposite bases, **D**s form base pairs with complementary bases, causing the nucleoside surrogate **P** to flip outside the DNA helix and strengthening the fluorescence intensity of **P**. On the other hand, when the mismatched bases have sites opposite of **D**s, **P** intercalates into the DNA helix because the tricyclic base-linked nucleoside surrogate **P** is more intercalative than natural mono or bicyclic natural nucleobases. This weakens the fluorescence intensity of **P**. We anticipated that we could determine the type of nucleobase involved in the SNP site by comparing the fluorescence intensities of duplexes composed of each probe containing **P**.

2. Results

2.1. Design and synthesis of a fluorescent nucleoside surrogate

Size-expanded nucleoside surrogates **2** and **3** were reported fluoresce under ultraviolet light, emitting fluorescence at ~400 nm.[24–27] Thus, we chose 8-amino-3-(2,3-dihydroxypropyl)imidazo[4′,5′:5,6]pyrido[2,3-*d*]pyrimidine (**P**) as a nucleoside surrogate for this method. We expected that the nucleoside surrogate **P** could be accommodated into a DNA/DNA or DNA/RNA helix without disturbing the local helical structure because **P** is composed of an acyclic three-carbon propylene glycol instead of deoxy-D-ribose, although it carries a size-expanded tricyclic base. We also expected that **P** would flip outside of the helix more easily than natural nucleosides because **P** has a flexible acyclic structure.

The synthesis of the tricyclic base-linked nucleoside surrogate **P** is shown in Scheme 1. 5-Amino-6-cyanoimidazo[4,5-*b*]pyridine (**4**),[28] which was synthesized by a method reported previously, was coupled with (*R*)-2,2-dimethyl-4-(*p*-toluenesulfonyloxymethyl)-1,3-dioxolane (**5**) in the presence of K_2CO_3 in dimethylformamide (DMF) at 60 °C. Only one product was observed on thin-layer chromatography (TLC). After purification on a silica gel column, the product was analyzed by ^1H–^1H correlation spectroscopy (COSY), heteronuclear multiple quantum coherence (HMQC), heteronuclear multiple bond correlation (HMBC) and nuclear overhauser enhancement spectroscopy (NOESY) spectra. In the NOESY experiments, cross-peaks were observed between H2 of the base moiety and the protons of the 1,3-dioxolanylmethyl residue, but no cross-peak was detected between H7 of the base moiety and the 1,3-dioxolanylmethyl portion. From these results, the product was identified as an N3-alkyl derivative **6**. Treatment of **6** with $CH(OEt)_3$ at 100 °C followed by treatment with methanolic ammonia in a steel sealed tube at 110 °C produced an isopropylidene derivative of **P**. The amino group of **7** was protected with a benzoyl group. Deprotection of the isopropylidene group, protection of the primary hydroxy group with 4,4′-dimethoxytrityl (DMTr) group, and phosphitylation produced phosphoramidite unit **12**.

2.2. Photophysical properties of the nucleoside surrogate P

Typical emission spectra of the tricyclic base-linked nucleoside surrogate **P** are shown in Fig. 3. The nucleoside surrogate **P** showed emission maxima at ~390 nm under 332-nm excitation. The fluorescence intensity of **P** depended on solvent polarity; fluorescence intensity of **P** was greater in more polar solvents such as methanol and water compared to less polar solvents such as chloroform. The photophysical data of the tricyclic base-linked nucleoside surrogate **P** are summarized in Table 1. The emission wavelength of **P** was affected by solvent polarity. The emission maximum shifted from 388 nm for chloroform to 399 nm for methanol. The fluorescence quantum yields (Φs) of **P** increased with increasing solvent polarity. The Φ value of **P** was 0.13 in chloroform and 0.97 in water.

2.3. Synthesis of ODNs containing the nucleoside surrogate P

The sequences of ODNs containing the nucleoside surrogate **P** are given in Table 2. CYP2C9 is one of the predominant cytochrome P450 (CYP) enzymes expressed constitutively in the human liver.[29,30] It metabolizes a variety of therapeutically important drugs such as phenytoin, warfarin, and a number of anti-inflammatory drugs, including indomethacin, mefenamic acid, flurbiprofen, ibuprofen, diclofenac, and the oxicams.[29,30] In the present study, we chose the sequence containing an A1075(C) mutation in the *CYP2C9* gene as a model sequence. The probe ODNs were composed of sequences complementary to the *CYP2C9* gene. The probes (5′-P-probes) termed **PA**, **PG**, **PC**, and **PT** contained **P** at the 5′ sides of **D**s, whereas the probes (3′-P-probes) termed **AP**, **GP**, **CP**, and **TP** possessed **P** at the 3′ sides of **D**s. Target sequences are abbreviated as S.

All the ODNs containing **P** were synthesized using a DNA/RNA synthesizer. Fully protected ODNs (1.0 μmol each) linked to solid supports were treated with concentrated NH_4OH at 55 °C for 12 h. The ODNs released after treatment were purified by 20% polyacrylamide gel electrophoresis (PAGE) to afford deprotected ODNs. These ODNs were analyzed by MALDI-TOF/MS, and the observed molecular weights were in agreement with their structures.

2.4. Thermal denaturation study and fluorescence experiments of duplexes containing P

First, we examined the ability of the probes to detect SNPs in the DNA targets. The T_m values of the duplexes between the probes and the DNA targets are shown in Table 3 (left column). The highest T_m values were from the duplexes comprising complementary sequences, for example, when the discriminating bases and the target base sequences matched. ΔT_m variation between the matched and mismatched sequences was 3–7 °C. Thus, the discriminating bases possessed sufficient base-selectivity, although they contained the tricyclic nucleoside surrogate **P** at the 5′ or 3′ sides of the discriminating bases.

Fluorescence emission spectra of the duplexes consisting of 5′-P-probes, **PA**, **PG**, **PC**, and **PT** are shown in Fig. 4. Fluorescence

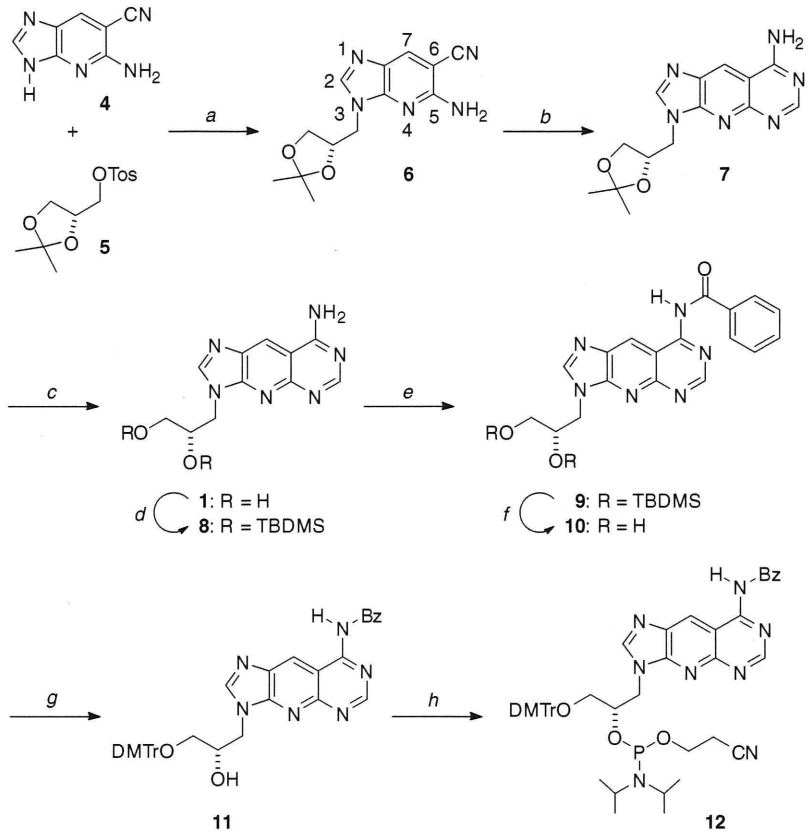

Scheme 1. Reagents and conditions: (a) K_2CO_3, DMF, 60 °C, 70 h, 54%; (b) $HC(OEt)_3$, 100 °C, 54 h; (2) NH_3 in MeOH, 110 °C, 18 h, 65%; (c) CH_3CO_2H, 60 °C, 9 h, 98%; (d) TBDMSCl, imidazole, DMF, rt, 18 h, 81%; (e) BzCl, pyridine, rt, 10 h, 67%; (f) TBAF, THF, rt, 2 h, 75%; (g) DMTrCl, pyridine, rt, 2 h, 56%; (h) chloro(2-cyanoethoxy)(*N*,*N*-diisopropylamino)phosphine, *i*-Pr_2NEt, THF, rt, 30 min, 67%.

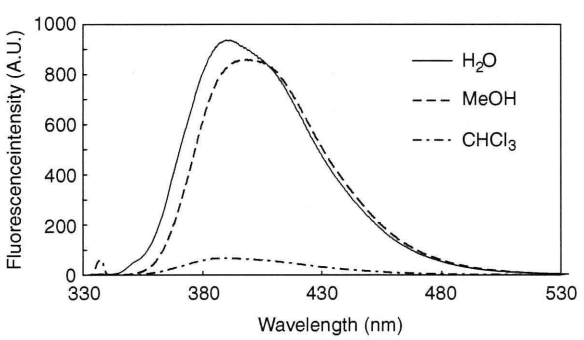

Figure 3. Fluorescence emission spectra of **P** in various solvents. Spectra were obtained under 332-nm excitation on a spectrofluorophotometer in quartz cuvettes with a path length of 1.0 cm at a **P** concentration of 30 μM in an appropriate solvent at 20 °C. Spectra were recorded using an excitation slit of 1.5 nm and emission slit of 1.5 nm.

Table 1
Photophysical properties of **P**. The experimental conditions were described in the Section 4

Solvent	λ_{ex} (nm)	λ_{em} (nm)	ε	Φ
H_2O	333.4	391.6	78.5	0.97
MeOH	335.4	398.6	32.6	0.82
CH_3CN	334.8	386.8	36.2	0.70
EtOAc	336.6	386.4	6.19	0.43
THF	338.8	389.8	7.32	0.19
$CHCl_3$	335.0	388.2	4.70	0.13
CH_2Cl_2	335.0	385.0	8.90	0.12

Φ = fluorescence quantum yield.
ε = dielectric constant.

spectra intensity of the duplexes correlated with the T_m values of the duplexes. In all sequences, the fluorescence intensities were greatest when the discriminating bases were complementary to the target bases. Next, we compared the fluorescence intensities of the duplexes at 390 nm. As shown in Fig. 5 (left column), the fluorescence intensities were greatest when the duplexes were composed of matched sequences: **PA** probe for the SdT target, **PC** probe for the SdG target, **PT** probe for the SdA target, and **PG** probe for the SdC target. However, with the dG target base, fluorescence was also observed for the **PT** probe. This was attributed to a wobble-type base pairing between dG and dT bases.[31] The fluorescence intensities of the single-stranded P-probes were almost equal to those of the mismatched duplexes (data not shown).

The results for probes containing the surrogate **P** at the 3′ side of the discriminating bases (3′-P-probes) are shown in Fig. 6 (left column). Fluorescence intensities of the duplexes were greatest when the discriminating bases were complementary to the target bases (except for the **CP** probe): **AP** probe for the SdT target, **TP** probe for the SdA target, and **GP** probe for the SdC target. No fluorescence was observed with the **CP** probe for the target sequences. From these results, we could determine the type of nucleobases involved in the SNP sites in the DNA targets using the **PA** or **AP** probe for the SdT target, the **PC** probe for the SdG target, the **TP** probe for the SdA target, and the **PG** probe for the SdC target.

Table 2
Oligonucleotide sequences. The underlined letters indicate discriminating bases. The italic letters represent target bases

Abbreviation	Sequence
PA	5′-d(GAA GGT CAA **P**A̲G TAT CTC T)-3′
PG	5′-d(GAA GGT CAA **P**G̲G TAT CTC T)-3′
PC	5′-d(GAA GGT CAA **P**C̲G TAT CTC T)-3′
PT	5′-d(GAA GGT CAA **P**T̲G TAT CTC T)-3′
PsT	5′-d(GAA GGT CAA **P**s̲TG TAT CTC T)-3′
AP	5′-d(GAA GGT CAA A̲**P**G TAT CTC T)-3′
GP	5′-d(GAA GGT CAA G̲**P**G TAT CTC T)-3′
CP	5′-d(GAA GGT CAA C̲**P**G TAT CTC T)-3′
TP	5′-d(GAA GGT CAA T̲**P**G TAT CTC T)-3′
SdA	3′-d(CTT CCA GTT *A*CA TAG AGA)-5′
SdG	3′-d(CTT CCA GTT *G*CA TAG AGA)-5′
SdC	3′-d(CTT CCA GTT *C*CA TAG AGA)-5′
SdT	3′-d(CTT CCA GTT *T*CA TAG AGA)-5′
SrA	3′-r(CUU CCA GUU *A*CA UAG AGA)-5′
SrG	3′-r(CUU CCA GUU *G*CA UAG AGA)-5′
SrC	3′-r(CUU CCA GUU *C*CA UAG AGA)-5′
SrU	3′-r(CUU CCA GUU *U*CA UAG AGA)-5′

Table 3
T_m Values. ΔT_ms [T_m (a duplex between a probe and a complementary target) − T_m (a duplex between a probe and a target containing a mismatched base)] are indicated in parentheses. The experimental conditions are as described in the Section 4

	SdA	SdG	SdC	SdT	SrA	SrG	SrC	SrU
PA	45.6 (−4.5)	47.8 (−2.3)	44.9 (−5.1)	50.1 –	45.0 (−3.1)	47.1 (−1.0)	44.6 (−3.5)	48.1 –
PG	45.8 (−5.8)	45.8 (−5.8)	51.6 –	46.8 (−3.8)	46.8 (−5.5)	47.8 (−4.5)	52.3 –	46.9 (−5.4)
PC	44.5 (−5.6)	52.1 –	44.6 (−5.5)	46.1 (−6.0)	45.5 (−7.7)	51.5 –	44.9 (−6.6)	45.7 (−5.5)
PT	50.5 –	47.1 (−3.4)	45.7 (−4.8)	47.3 (−3.2)	49.2 –	48.0 (−1.2)	44.8 (−4.4)	47.0 (−2.2)
AP	47.8 (−2.5)	46.8 (−3.5)	46.4 (−3.9)	50.3 –	46.5 (−1.4)	49.6 (+1.7)	46.1 (−1.8)	47.9 –
GP	49.1 (−3.5)	47.2 (−5.4)	52.6 –	48.3 (−4.3)	48.1 (−4.7)	48.7 (−4.1)	52.8 –	47.4 (−5.4)
CP	49.8 (−5.1)	54.9 –	48.0 (−6.9)	49.1 (−5.8)	47.2 (−8.9)	56.1 –	48.0 (−8.1)	49.3 (−6.8)
TP	52.4 –	48.9 (−3.5)	47.7 (−4.7)	49.4 (−3.0)	50.0 –	51.7 (+1.7)	48.2 (−2.1)	48.9 (−1.1)

The results for the RNA targets are shown in Table 3 (right column), Fig. 5 (right column), and Fig. 6 (right column). When the discriminating bases and the target bases matched, the T_m values of the duplexes were greatest in all sequences, except for the **AP** and **TP** probes, whose ΔT_m values for duplexes comprising matched and mismatched sequences varied from 1 to 9 °C. Thus, the discriminating bases seemed to have base selectivities in the DNA/RNA duplexes containing the tricyclic nucleoside surrogate **P**. The T_m values of the **AP**/SrG (T_m = 49.6 °C) and **TP**/SrG (T_m = 51.7 °C) duplexes were slightly greater than those of the **AP**/SrU (T_m = 47.9 °C) and **TP**/SrA (T_m = 50.0 °C) duplexes, which were complementary. These differences in the T_m values were attributed to sheared G:A base pairing[32,33] and a wobble-type base pairing between dG and dT bases.[31]

The results of the fluorescence experiment for the RNA targets were similar to those for the DNA targets. The fluorescence intensities of the duplexes containing the 5′-P-probes were greatest when the discriminating bases were complementary to the target bases, except for the PT/SrG duplex (Fig. 5, right column). The fluorescence of the mismatched PT/SrG duplex was attributed to the wobble-type base pairing between dT and rG bases. Results for the 3′-P-probes are shown in Figure 6 (right column). The fluorescence intensities were greatest when the duplexes were complementary, although the fluorescence intensities of the duplexes composed of the **CP** probe were weak in all target sequences. However, in principle, we could determine the type of nucleobases involved in the SNP sites in the RNA target using four 5′-P-probes or four 3′-P-probes.

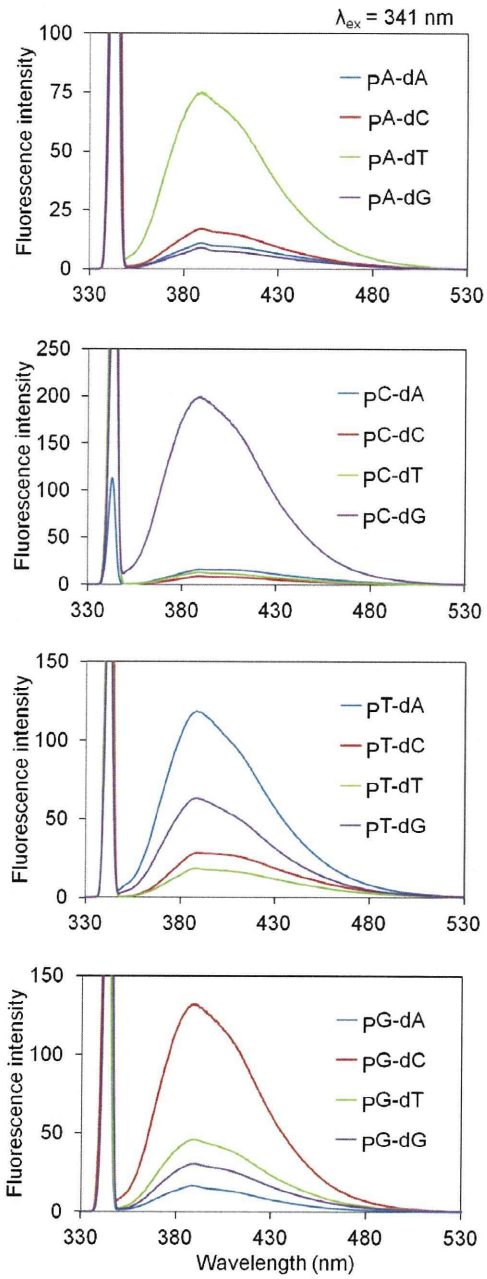

Figure 4. Fluorescence emission spectra of the duplexes. Spectra were obtained under 341-nm excitation on a spectrofluorophotometer in quartz cuvettes with a path length of 1.0 cm and a duplex concentration of 3.0 μM in a T_m buffer at 20 °C. Spectra were recorded with using an excitation slit of 1.5 nm and emission slit of 1.5 nm.

To improve sensitivity and solve the problem related to wobble-type base pairing, we designed and synthesized a probe containing 2-thiothymidine (sT) as a discriminating base. Sekine et al. reported that the formation of wobble-type base pairing between dG and dT can be suppressed by introducing a thiocarbonyl group into the 2-position of dT instead of a 2-carbonyl oxygen (Fig. 7).[34]

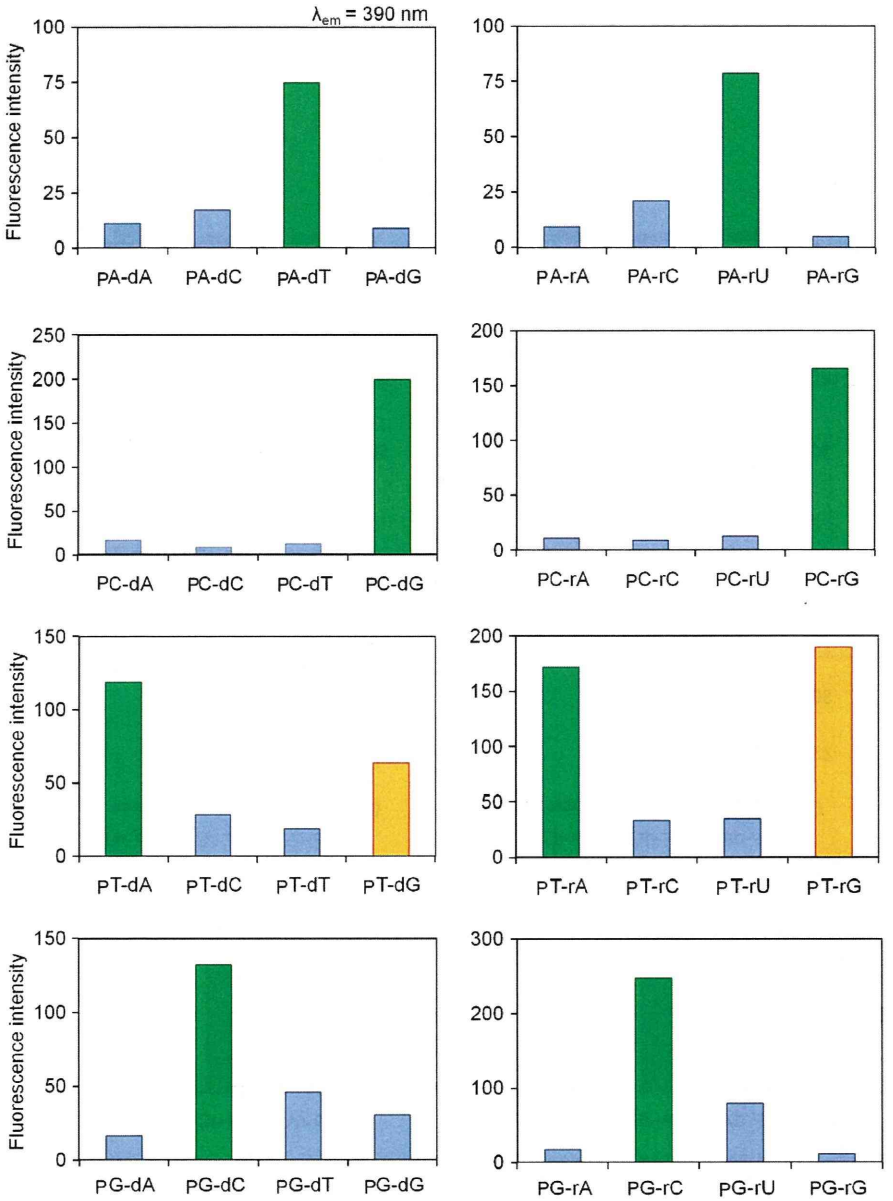

Figure 5. Fluorescence intensities of duplexes at 390 nm. Left column: 5′-P-probe/DNA target. Right column: 5′-P-probe/RNA target. Spectra were measured at 20 °C.

Therefore, we expected that fluorescence due to the formation of wobble-type base pairing could be suppressed by introducing sT instead of dT (Table 2). The results of fluorescence experiments are shown in Fig. 8. The left graph shows the result of the DNA target, while the right graph represents the result of the RNA target. Fluorescence due to the formation of wobble-type base pairing was reduced by introducing sT instead of dT without affecting other base pairings.

3. Discussion and conclusions

A reliable and simple method for detecting nucleotide mutations is very important clinically because sequence variations in human DNA cause genetic diseases and genetically influenced traits. The majority of sequence variations are attributed to SNPs.[1,2] In this study, we developed a novel method for SNP detection. The fluorescence intensity of the nucleoside surrogate **P**, a key compound in this system, depended on solvent polarity. When the probe containing **P** hybridized with a complementary sequence, the probe emitted fluorescence. However, when the probe hybridized with a target containing a mismatched base, the probe did not fluoresce in the almost sequences. Thus, in principle, we can identify the kind of nucleotide involved in an SNP site using 4 probes containing only 1 nucleoside surrogate **P**.

The fluorescence intensity values varied significantly even when the duplex types were the same. For example, the values obtained for the **PA**/SdT and **PC**/SdG duplexes, both of which are successful probes, were 75 and 200, respectively. Similarly, the values obtained for the **PA**/SrU and **PC**/SrG duplexes were 75 and 160. These phenomena may partly reflect the influence of the number of hydrogen bonding between the discriminating bases **D**s and the target bases. The dA:dT base pairing is formed by 2 hydrogen bonds, whereas the base pairing between dG and dC is composed of 3 hydrogen bonds. Thus, when the dG:dC base pair is formed between the discriminating base **D** and the target base, the nucleoside surrogate **P** may flip outside of the DNA helix more largely

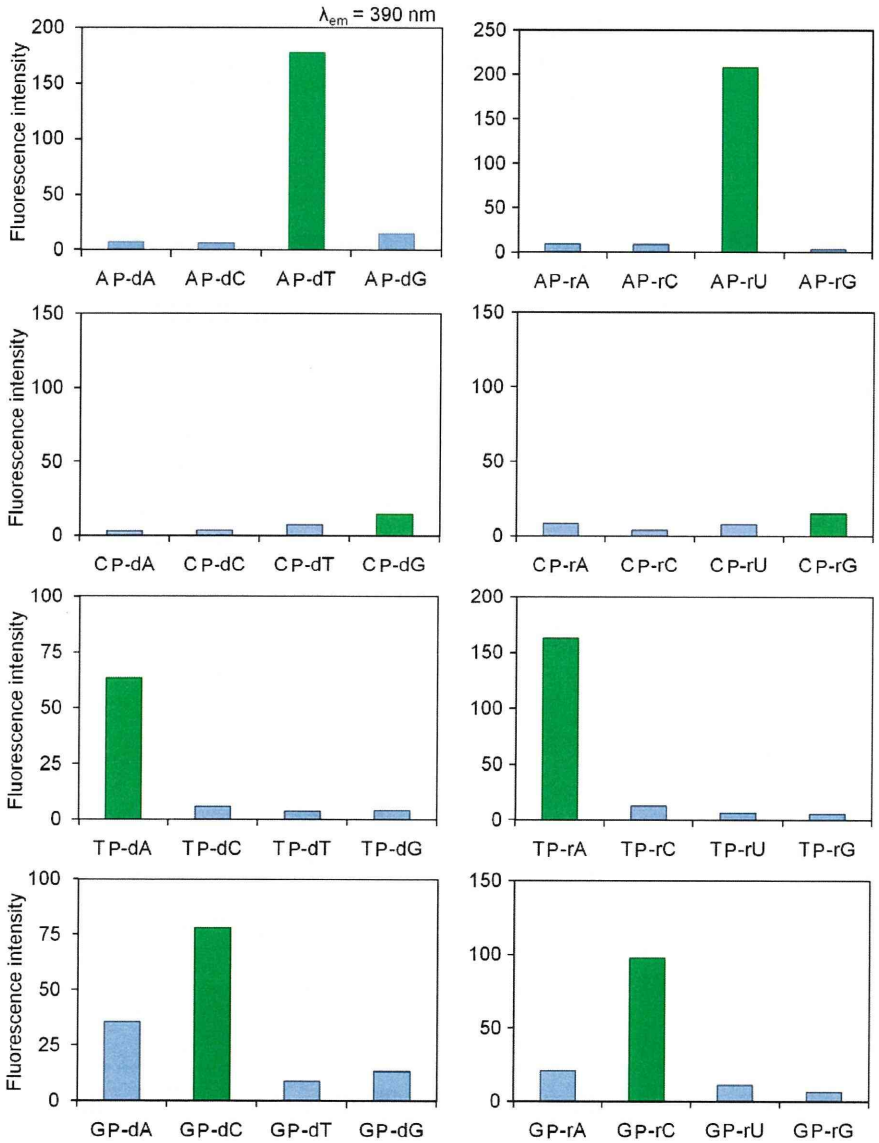

Figure 6. Fluorescence intensities of duplexes at 390 nm. Left column: 3′-P-probe/DNA target. Right column: 3′-P-probe/RNA target. Spectra were measured at 20 °C.

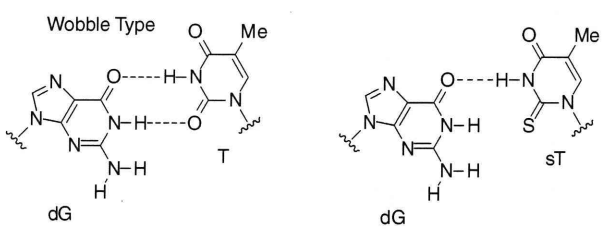

Figure 7. Base pairing between dG and T and between dG and 2-thiothymidine (sT).

as compared with the case of the dA:dT base pair: this may allow the nucleoside surrogate **P** to emit more fluorescence than the case of the dA:dT base pair.

Fluorescence signal patterns of the DNA and RNA target duplexes were not significantly different. Thus, global conformation differences between the duplexes, that is, B-type and A-type conformations, did not influence probe fluorescence intensity. In contrast, the position of the nucleoside surrogate **P** within the probes affected the fluorescence intensity of the duplexes. For example, the **PC** probe (5′-P-probe) worked well for detecting SNPs for the DNA and RNA targets, whereas the **CP** probe (3′-P-probe) did not emit fluorescence even when it hybridized with complementary targets. It is known that a guanine base can form not only a Watson–Crick base pairing with a cytosine base but also a sheared-type base pairing with an adenine base.[32,33] The base moiety of the nucleoside surrogate **P** has a proton donor–acceptor pattern same as adenosine. Thus, the nucleoside surrogate **P** might form a base pairing with the target dG or rG base like as the sheared-type base pairing in the **CP**/SdG or **CP**/SrG duplex. In this study, we tested only one sequence. In the future, we will systematically examine a large number of target sequences to confirm the general applicability of this system.

Fluorescence attributed to wobble-type T:G base pairing was observed for the **PT** probe (5′-P-probe), while the **TP** probe (3′-P-probe) worked well for detecting SNPs for both DNA and RNA targets. These results imply that the geometry of the nucleoside surrogate **P** in the duplexes was different in the 3′-P-probe and

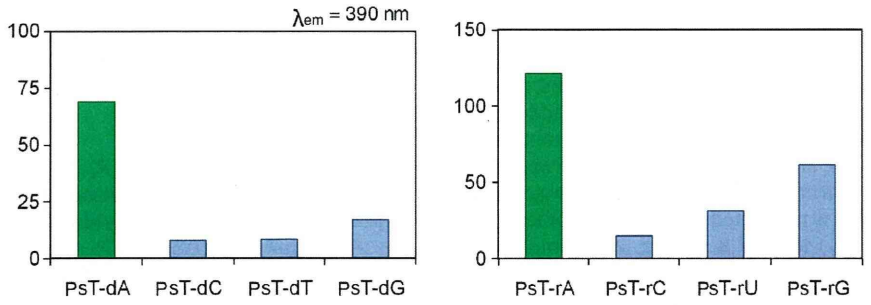

Figure 8. Fluorescence intensities of duplexes containing 2-thiothymidine (sT) at 390 nm. Spectra were measured at 20 °C.

the 5′-P-probe. Furthermore, intensity differences between the fluorescence signals of the matched and mismatched sequences were dependent on the kind of probe and the target sequences. The **AP**, **PC**, and **TP** probes worked well as SNP-detecting probes. When they hybridized with complementary targets, the fluorescence intensities of the duplexes increased 5- to 20-fold as compared to those with mismatched sequences.

As mentioned-above, it is known that a guanine base can form not only a Watson–Crick base pairing with a cytosine base but also a wobble-type base pairing with a thymine base and a sheared-type base pairing with an adenine base.[31–33] In this study, we observed fluorescence signals attributed to wobble-type G:T base pairing. We succeeded in reducing these fluorescence signals by introducing sT instead of dT in the probe. Furthermore, when the **GP** probe hybridized with the SdA target, fluorescence signal intensity increased slightly in comparison to other mismatched targets. This was attributed to sheared-type G:A base pairing. Introducing a chemically modified guanine base might solve the problem and improve the sensitivity of the probe.

In conclusion, we demonstrated the synthesis of DNA containing a fluorescent tricyclic base-linked acyclonucleoside **P**. We examined the properties of the DNA containing **P** as an SNP-detecting probe. We found that, in principle, we can determine the types of nucleobases involved in the SNP sites in DNA and RNA targets with high sensitivities using 4 probes containing **P**. Thus, this system would provide a novel and simple method for detecting SNPs in DNA and RNA targets although we must optimize the linker length and the structure of the base moiety. Synthesis of other fluorescent base-linked acyclonucleosides with distinct emission wavelengths are under investigation in our laboratory.

4. Experimental section

4.1. General remarks

Thin-layer chromatography was carried out on Merck coated plates $60F_{254}$. Silica gel column chromatography was carried out on Wakogel C-300. ^{1}H-, ^{13}C-, and ^{31}P NMR spectra were obtained with a JEOL JNM AL-400 spectrometer. $CDCl_3$ (CIL) or DMSO-d_6 (CIL) was used as a solvent for obtaining NMR spectra. Chemical shifts (δ) are given in parts per million (ppm) downfield from $(CH_3)_4Si$ (δ 0.00 for ^{1}H NMR in $CDCl_3$), 80% H_3PO_4 (δ 0.00 for ^{31}P NMR), or a solvent (for ^{13}C NMR and ^{1}H NMR in DMSO-d_6) as an internal reference with coupling constants (J) in Hz. The abbreviations s, d, and q signify singlet, doublet, and quartet, respectively.

4.1.1. (*S*)-5-Amino-6-cyano-3-[(2,2-dimethyl-1,3-dioxolan-4-yl) methyl]imidazo[4,5-*b*]pyridine (6)

A mixture of (*R*)-2,2-dimethyl-4-(*p*-toluenesulfonyloxymethyl)-1,3-dioxolane (1.70 g, 5.94 mmol), 5-amino-6-cyanoimdazo[4,5-*b*]pyridine (0.76 g, 4.77 mmol),[28] and K_2CO_3 (0.80 g, 5.79 mmol) in DMF (80 mL) was stirred at 60 °C for 70 h. The mixture was partitioned between EtOAc and H_2O. The organic layer was washed with brine, dried (Na_2SO_4), and concentrated. The residue was purified by column chromatography (SiO_2, 1–2% MeOH in $CHCl_3$) to give **6** (0.70 g, 2.56 mmol) in 54% yield: ^{1}H NMR (400 MHz, DMSO-d_6) δ 1.33 (s, 3H, 2-C*H*$_3$), 1.38 (s, 3H, 2-C*H*$_3$), 3.71 (dd, 1H, J = 6.0 and 8.7, 5-C*H*$_a$H$_b$), 4.11 (dd, 1H, J = 6.5 and 8.7, 5-CH$_a$*H*$_b$), 4.19 (dd, 1H, J = 6.0 and 14.5, NC*H*$_a$H$_b$), 4.32 (dd, 1H, J = 3.6 and 14.5, NCH$_a$*H*$_b$), 4.46 (m, 1H, 4-C*H*), 5.11 (s, 2H, 5-N*H*$_2$), 7.97 (s, 1H, 2-*H*), 8.07 (s, 1H, 7-*H*); ^{13}C NMR (100 MHz, DMSO-d_6) δ 24.9, 26.4, 45.0, 65.8, 72.9, 85.3, 108.5, 117.3, 125.9, 133.3, 144.1, 148.6, 156.9; HRMS (FAB) calcd for $C_{13}H_{15}N_5O_2$: 273.1226, found; 273.1229. Anal. Calcd for $C_{13}H_{16}N_6O_2 \cdot 11/50H_2O$: C, 56.32; H, 5.61; N, 25.26. Found: C, 56.58; H, 5.47; N, 24.96.

4.1.2. (*S*)-8-Amino-3-[(2,2-dimethyl-1,3-dioxolan-4-yl) methyl]imidazo[4′,5′:5,6]pyrido[2,3-*d*]pyrimidine (7)

A solution of **6** (1.20 g, 4.39 mmol) in triethyl orthofomate (40 mL, 240 mmol) was stirred at 100 °C for 54 h, cooled to room temperature, and concentrated. The residue was dissolved in saturated NH_3/MeOH (50 mL). The tube was sealed and the solution was stirred at 110 °C for 18 h. After cooling the mixture, the tube was opened and the excess NH_3 was allowed to escape slowly. The mixture was concentrated. The residue was purified by column chromatography (SiO_2, 6–10% MeOH in $CHCl_3$) to give **7** (0.86 g, 2.86 mmol) in 65% yield: ^{1}H NMR (400 MHz, DMSO-d_6) δ 1.22 (s, 3H), 1.27 (s, 3H), 3.82 (dd, 1H, J = 5.1 and 8.7), 4.06 (dd, 1H, J = 6.5 and 8.7), 4.39 (dd, 1H, J = 6.5 and 14.0), 4.47 (dd, 1H, J = 4.2 and 14.0), 4.56 (m, 1H), 7.99 (br s, 2H, D_2O exchangeable), 8.47 (s, 1H), 8.64 (s, 1H), 9.03 (s, 1H); ^{13}C NMR (100 MHz, DMSO-d_6) δ 25.0, 26.5, 45.4, 66.1, 73.3, 91.2, 106.0, 106.9, 109.0, 123.2, 150.3, 151.6, 157.4, 163.9; HRMS (FAB) calcd for $C_{14}H_{17}N_6O_2$: 301.1422, found; 301.1413. Anal. Calcd for $C_{14}H_{17}N_6O_2 \cdot 1/10H_2O$: C, 55.66; H, 5.44; N, 27.82. Found: C, 55.79; H, 5.42; N, 27.50.

4.1.3. (*S*)-8-Amino-3-[2,3-dihydroxypropyl]imidazo[4′,5′:5,6] pyrido[2,3-*d*]pyrimidine (1)

A solution of **7** (0.86 g, 2.86 mmol) in 80% CH_3CO_2H (30 mL) was stirred at 60 °C for 9 h. The solvent was evaporated in vacuo to give **1** (0.74 g, 2.83 mmol) in 98% yield: UV λ_{max} (H_2O) 260 nm (ε = 14700), 333 nm (ε = 18300); ^{1}H NMR (400 MHz, DMSO-d_6) δ 3.39 (m, 2H), 3.93 (m, 1H), 4.14 (dd, 1H, J = 8.7 and 13.9), 4.48 (dd, 1H, J = 3.4 and 14.0), 4.90 (t, 1H, J = 5.5), 5.14 (d, 1H, J = 5.9), 7.97 (br s, 2H), 8.47 (s, 1H), 8.59 (s, 1H), 9.01 (s, 1H); ^{13}C NMR (100 MHz, DMSO-d_6) δ 46.6, 63.7, 69.3, 105.8, 122.9, 134.0, 150.7, 151.6, 155.1, 157.3, 163.9; HRMS (FAB) calcd for $C_{11}H_{13}N_6O_2$: 261.1111, found; 261.1100. Anal. Calcd for $C_{11}H_{13}N_6O_2 \cdot 1/5\ H_2O$: C, 50.29; H, 4.74; N, 30.87. Found: C, 50.37; H, 4.87; N, 30.89.

4.1.4. (*S*)-8-Amino-3-[2,3-bis(*tert*-butyldimethylsilyloxy) propyl]imidazo[4′,5′:5,6]pyrido[2,3-*d*]pyrimidine (8)

A solution of **1** (0.75 g, 2.88 mmol), imidazole (1.75 g, 25.7 mmol), TBDMSCl (1.58 g, 10.5 mmol) in DMF (30 mL) was stirred at room temperature for 18 h. EtOH (1 mL) was added to the mixture, and the whole was stirred for 10 min. The mixture was partitioned between EtOAc and H_2O. The organic layer was washed with aqueous $NaHCO_3$ (saturated) and brine, dried (Na_2SO_4), and concentrated. The residue was purified by column chromatography (SiO_2, 3% MeOH in $CHCl_3$) to give **8** (1.14 g, 2.33 mmol) in 81% yield: ^{1}H NMR (400 MHz, DMSO-d_6) δ −0.63 (s, 3H), −0.15 (s, 3H), 0.08 (s, 6H), 0.65 (s, 9H), 0.90 (s, 9H), 3.66 (m, 2H), 4.26 (m, 2H), 4.47 (m, 1H), 7.98 (br s, 2H), 8.47 (s, 1H), 8.58 (s, 1H), 9.01 (s, 1H); ^{13}C NMR (100 MHz, DMSO-d_6) δ −5.9, −5.5, −5.4, −4.9, 17.4, 18.1, 25.5, 25.9, 46.7, 65.7, 70.4, 105.8, 123.0, 134.1, 150.6, 151.6, 155.2, 157.3, 163.9; HRMS (FAB) calcd for $C_{23}H_{40}N_6O_2Si_2$: 488.2751, found; 488.2760. Anal. Calcd for $C_{23}H_{40}N_6O_2Si_2$: C, 56.52; H, 8.25; N, 17.19. Found: C, 56.37; H, 8.10; N, 17.24.

4.1.5. (*S*)-N^8-Benzoylamino-3-[2,3-bis(*tert*-butyldimethylsilyl oxy)propyl]imidazo[4′,5′:5,6]pyrido[2,3-*d*]pyrimidine (9)

A solution of **8** (1.82 g, 3.72 mmol) and BzCl (0.64 mL, 5.51 mmol) in pyridine (20 mL) was stirred at room temperature. After 10 h, the mixture was partitioned between $CHCl_3$ and H_2O. The organic layer was washed with aqueous $NaHCO_3$ (saturated) and brine, dried (Na_2SO_4), and concentrated. The residue was purified by column chromatography (SiO_2, 0–10% MeOH in $CHCl_3$) to give **9** (1.48 g, 2.50 mmol) in 67% yield: ^{1}H NMR (400 MHz, $CDCl_3$) δ −0.47 (s, 3H), −0.08 (s, 3H), 0.07 (s, 6H), 0.78 (s, 9H), 0.92 (s, 9H), 3.61 (m, 1H), 3.70 (m, 1H), 4.23 (m, 1H), 4.37 (m, 1H), 4.67 (m, 1H), 7.51–7.57 (m, 3H), 8.37–8.48 (m, 4H), 9.53 (s, 1H); ^{13}C NMR (100 MHz, $CDCl_3$) δ −5.4, −5.3, −4.7, 17.8, 18.4, 25.7, 26.0, 47.4, 65.4, 70.7, 113.6, 126.9, 128.3, 130.0, 132.7, 135.9, 137.2, 143.6, 150.6, 152.6, 154.2, 159.0, 180.0. Anal. Calcd for $C_{23}H_{44}N_6O_3Si_2$: C, 60.77; H, 7.48; N, 14.09. Found: C, 60.51.; H, 7.40; N, 14.11.

4.1.6. (*S*)-N^8-Benzoylamino-3-[2,3-dihydroxypropyl]imidazo[4′, 5′:5,6]pyrido[2,3-*d*]pyrimidine (10)

A solution of **9** (1.48 g, 2.50 mmol) and TBAF (9.96 mL, 9.96 mmol, 1 M THF solution) in THF (50 mL) was stirred at room temperature. After 2 h, the solvent was evaporated in vacuo. The residue was purified by column chromatography (SiO_2, 5–14% MeOH in $CHCl_3$) to give **10** (0.68 g, 1.87 mmol) in 75% yield: ^{1}H NMR (400 MHz, DMSO-d_6) δ 3.41 (ddd, 1H, J = 5.5, 5.5 and 11.0), 3.48 (ddd, 1H, J = 5.5, 5.5 and 11.0), 3.97 (m, 1H), 4.21 (dd, 1H, J = 8.8 and 14.0), 4.55 (dd, 1H, J = 3.4 and 14.0), 4.92 (t, 1H, J = 5.5), 5.18 (d, 1H, J = 5.5), 7.54–8.38 (m, 7H), 8.76 (s, 1H); ^{13}C NMR (100 MHz, DMSO-d_6) δ 47.4, 64.3, 69.8, 125.6, 128.9, 129.7, 132.7 (multiple), 135.7 (multiple), 152.8; HRMS (FAB) calcd for $C_{18}H_{16}N_6O_3$: 365.1362, found; 365.1361. Anal. Calcd for $C_{18}H_{67}N_6O_3 \cdot 7/10H_2O$: C, 57.35; H, 4.65; N, 22.29. Found: C, 57.45; H, 4.73; N, 22.08.

4.1.7. (*S*)-N^8-Benzoylamino-3-[3-(4,4′-dimethoxytrityloxy)-2-hydroxypropyl]imidazo[4′,5′:5,6]pyrido[2,3-*d*]pyrimidine (11)

A solution of **10** (0.60 g, 1.65 mmol) and DMTrCl (0.84 g, 2.48 mmol) in pyridine (6 mL) was stirred at room temperature. After 2 h, the mixture was partitioned between $CHCl_3$ and H_2O. The organic layer was washed with aqueous $NaHCO_3$ (saturated) and brine, dried (Na_2SO_4), and concentrated. The residue was purified by column chromatography (SiO_2, 1% MeOH in $CHCl_3$) to give **11** (0.62 g, 0.93 mmol) in 56% yield: ^{1}H NMR (400 MHz, $CDCl_3$) δ 3.09 (m, 1H), 3.17 (dd, 1H, J = 6.3 and 9.9), 3.31 (dd, 1H, J = 4.4 and 9.9), 4.29 (m, 1H), 4.42 (dd, 1H, J = 7.5 and 14.4), 4.63 (dd, 1H, J = 3.2 and 14.4), 6.08–6.82 (m, 4H), 7.22–7.31 (m, 7H), 7.34–7.41 (m, 2H), 7.51–7.60 (m, 3H), 8.40 (m, 2H), 8.48 (m, 2H), 9.52 (s, 1H); ^{13}C NMR (100 MHz, $CDCl_3$) δ 47.6, 55.3, 64.9, 69.0, 86.6, 113.3, 126.4, 127.1, 127.3, 128.0, 128.1, 128.4, 130.0, 130.1, 132.7, 135.4, 135.6, 135.7, 144.6, 150.5, 152.3, 158.7. Anal. Calcd for $C_{39}H_{34}N_6O_5 \cdot 9/5H_2O$: C, 67.00; H, 5.42; N, 12.02. Found: C, 67.34; H, 5.08; N, 11.63.

4.1.8. N^8-Benzoylamino-3-[(*R*)-3-(4,4′-dimethoxytrityloxy) -2-[[(2-cyanoethoxy)(*N*,*N*-diisopropylamino)phosphanyl]oxy] -propyl]imidazo[4′,5′:5,6]pyrido[2,3-*d*]pyrimidine (12)

A solution of 11 (0.50 g, 0.75 mmol), *N*,*N*-diisopropylethylamine (0.65 mL, 3.74 mmol), and chloro(2-cyanoethoxy)(*N*,*N*-diisopropylamino)phosphine (0.33 mL, 1.48 mmol) in THF (4 mL) was stirred at room temperature. After 30 min, the mixture was partitioned between $CHCl_3$ and H_2O. The organic layer was washed with aqueous $NaHCO_3$ (saturated) and brine, dried (Na_2SO_4), and concentrated. The residue was purified by column chromatography (SiO_2, 50% EtOAc in hexane) to give **12** (0.43 g, 0.50 mmol) in 67% yield: ^{31}P NMR (162 MHz, DMSO-d_6) δ 149.1, 150.2.

4.2. Oligonucleotide synthesis

The synthesis was carried out with a DNA/RNA synthesizer (Applied Biosystems Model 3400) by the phosphoramidite method. In the case of the coupling of the amidite **12**, a 0.12 M solution of the amidite **12** in CH_3CN and a coupling time of 15 min were used. Deprotection of the bases and phosphates was performed in concentrated NH_4OH at 55 °C for 16 h. The oligonucleotides were purified by 20% PAGE containing 7 M urea to give the highly purified oligonucleotides, **PA** (14), **PG** (40), **PC** (20), **PT** (8), **AP** (15), **GP** (15), **CP** (14), **TP** (29), and **PsT** (15). The yields are indicated in parentheses as OD units at 260 nm starting from 1.0 μmol scale. The extinction coefficients of the oligonucleotides were calculated from those of mononucleotides and dinucleotides according to the nearest-neighbor approximation method.[35]

4.3. MALDI-TOF/MS analyses of oligonucleotides

Spectra were obtained with a SHIMADZU AXIMA-CFR plus time-of-flight mass spectrometer equipped with a nitrogen laser (337 nm, 3-ns pulse). A solution of 3-hydroxypicolinic acid (3-HPA) and diammonium hydrogen citrate in H_2O was used as the matrix. **PA**: calculated mass, 5844.8; observed mass, 5846.2. **PG**: calculated mass, 5860.8; observed mass, 5856.2. **PC**: calculated mass, 5820.8; observed mass, 5823.8. **PT**: calculated mass, 5835.8; observed mass, 5833.0. **AP**: calculated mass, 5844.8; observed mass, 5843.6. **GP**: calculated mass, 5860.8; observed mass, 5862.2. **CP**: calculated mass, 5820.8; observed mass, 5823.0. **TP**: calculated mass, 5835.8; observed mass, 5837.1. **PsT**: calculated mass, 5851.7; observed mass, 5851.1.

4.4. Absorption experiments

Absorption spectra (200–500 nm) were obtained on a SHIMAZU UV-2450 UV–Vis spectrophotometer in quartz cuvettes with a path length of 1.0 cm and a 30 μM **P** concentration in an appropriate solvent.

4.5. Thermal denaturation study

The solution containing the duplex in a buffer comprising 10 mM sodium phosphate (pH 7.0) and 0.1 M NaCl was heated at 95 °C for 3 min, cooled gradually to an appropriate temperature, and then used for the thermal denaturation study. The thermal-induced transition of each mixture was monitored at 260 nm on a SHIMAZU UV-2450 UV–Vis spectrophotometer fitted with a temperature controller in quartz cuvettes with a path length of

1.0 cm and a 3.0 μM duplex concentration in a buffer of 10 mM sodium phosphate (pH 7.0) and 0.1 M NaCl. The sample temperature was increased by 0.5 °C/min.

4.6. Fluorescence experiments

Steady-state fluorescence emission spectra (370–670 nm) were obtained on a SHIMADZU RF-5300PC spectrofluorophotometer in quartz cuvettes with a path length of 1.0 cm and a 30 μM **P** concentration in an appropriate solvent or a 3.0 μM duplex concentration in a T_m buffer at 20 °C. Spectra were recorded with use of excitation slit of 1.5 nm and emission slit of 1.5 nm for **P** or excitation slit of 3.0 nm and emission slit of 3.0 nm for the duplexes. The fluorescence quantum yield (Φ_{em}) was determined by use of quinine as a reference with the known Φ_{em} value of 0.58 (22 °C) in 0.1 M H_2SO_4. The quantum yield was calculated according to the following equation: $\Phi_{em(S)}/\Phi_{em(R)} = (I_{(S)}/I_{(R)}) \times (A_{(S)}/A_{(R)}) \times (n_{(S)}{}^2/n_{(R)}{}^2)$. Here, $\Phi_{em(S)}$ and $\Phi_{em(R)}$ are the fluorescence quantum yields of the sample and the reference, respectively, $I_{(S)}$ and $I_{(R)}$ are the integrated fluorescence intensities of the sample and the reference, respectively, $A_{(S)}$ and $A_{(R)}$ are the respective optical density of the sample and the reference solutions at the wavelength of excitation, and $n_{(S)}{}^2$ and $n_{(R)}{}^2$ are the values of the refractive index for the respective solvents.

Acknowledgments

This study was supported in part by a Grant-in-Aid from Precursory Research for Embryonic Science and Technology (PRESTO) of Japan Science and Technology (JST), a Grant-in-Aid from the Koshiyama Research Grand and a Grant-in-Aid for Scientific Research (C) from the Japan Society for the Promotion of Science (JSPS) to Y.U.

Supplementary data

Supplementary data associated with this article can be found, in the online version, at doi:10.1016/j.bmc.2011.11.045.

References and notes

1. Sachidanandam, R.; Weissman, D.; Schmidt, S. C.; Kakol, J. M.; Stein, L. D.; Marth, G.; Sherry, S.; Mullikin, J. C.; Mortimore, B. J.; Willey, D. L., et al *Nature* **2001**, *409*, 928.
2. Venter, J. C.; Adams, M. D.; Myers, E. W.; Li, P. W.; Mural, R. J.; Sutton, G. G.; Smith, H. O.; Yandell, M.; Evans, C. A.; Holt, R. A., et al *Science* **2001**, *291*, 1304.
3. McCarthy, J. J.; Hilfiker, R. *Nat. Biotechnol.* **2000**, *18*, 505.
4. Wang, D. G.; Fan, J.-B.; Siao, C.-J.; Berno, A.; Young, P.; Sapolsky, R.; Ghandour, G.; Perkins, N.; Winchester, E.; Spencer, J., et al *Science* **1998**, *280*, 1077.
5. Hoheisel, J. D. *Nat. Rev. Genet.* **2006**, *7*, 200.
6. Hardenbol, P.; Baner, J.; Jain, M.; Nilsson, M.; Namsaraev, E. A.; Karlin-Neumann, G. A.; Fakhrai-Rad, H.; Ronaghi, M.; Willis, T. D.; Landegren, U.; Davis, R. W. *Nat. Biotechnol.* **2003**, *21*, 673.
7. Holland, P. M.; Abramson, R. D.; Watson, R.; Gelfand, D. H. *Proc. Natl. Acad. Sci. U.S.A.* **1991**, *88*, 7276.
8. Pourmand, N.; Elahi, E.; Davis, R. W.; Ronaghi, M. *Nucleic Acids Res.* **2002**, *30*, e31.
9. Lindroos, K.; Liljedahl, U.; Raitio, M.; Syvanen, A.-C. *Nucleic Acids Res.* **2001**, *29*, e69.
10. Ross, P.; Hall, L.; Smirnov, I.; Haff, L. *Nat. Biotechnol.* **1998**, *16*, 1347.
11. Stoerker, J.; Mayo, J. D.; Tetzlaff, C. N.; Sarracino, D. A.; Schwope, I.; Richert, C. *Nat. Biotechnol.* **2000**, *18*, 1213.
12. Okamoto, A.; Tanaka, K.; Saito, I. *J. Am. Chem. Soc.* **2003**, *125*, 4972.
13. Okamoto, A.; Tanaka, K.; Fukuta, T.; Saito, I. *J. Am. Chem. Soc.* **2003**, *125*, 9296.
14. Okamoto, A.; Kanatani, K.; Saito, I. *J. Am. Chem. Soc.* **2004**, *126*, 4820.
15. Saito, Y.; Hanawa, K.; Motegi, K.; Omoto, K.; Okamoto, A.; Saito, I. *Tetrahedron Lett.* **2005**, *46*, 7605.
16. Okamoto, A.; Tainaka, K.; Unzai, T.; Saito, I. *Tetrahedron* **2007**, *63*, 3465.
17. Tainaka, K.; Tanaka, K.; Ikeda, S.; Nishiza, K.; Unzai, T.; Fujiwara, Y.; Saito, I.; Okamoto, A. *J. Am. Chem. Soc.* **2007**, *129*, 4776.
18. Köhler, O.; Seitz, O. *Chem. Commun.* **2003**, 2938.
19. Köhler, O.; Jarikote, D. V.; Seitz, O. *ChemBioChem* **2005**, *6*, 69.
20. Jarikote, D. V.; Krebs, N.; Tannert, S.; Röder, B.; Seitz, O. *Chem. Eur. J.* **2007**, *13*, 300.
21. Bethge, L.; Jarikote, D. V.; Seitz, O. *Bioorg. Med. Chem.* **2008**, *16*, 114.
22. Bethge, L.; Singh, I.; Seitz, O. *Org. Biomol. Chem.* **2010**, *8*, 2439.
23. Young, M. A.; Jayaram, B.; Beveridge, D. L. *J. Phys. Chem. B* **1998**, *102*, 7666.
24. Dvorakova, H.; Holy, A.; Masojidkova, M. *Collect. Czech. Chem. Commun.* **1988**, *53*, 1779.
25. Clayton, R.; Davis, M. L.; Fraser, W.; Li, W.; Ramsden, C. A. *Synlett* **2002**, 1483.
26. Liu, H.; Gao, J.; Lynch, S. R.; Saito, Y. D.; Maynard, L.; Kool, E. T. *Science* **2003**, *302*, 868.
27. Liu, H.; Gao, J.; Maynard, L.; Saito, Y. D.; Kool, E. T. *J. Am. Chem. Soc.* **2004**, *126*, 1102.
28. Harris, P. A.; Pendergast, W. *J. Heterocycl. Chem.* **1996**, *33*, 319.
29. Rettie, A. E.; Wienkers, L. C.; Gonzalez, F. J.; Trager, W. F.; Korzekwa, K. R. *Pharmacogenetics* **1994**, *4*, 39.
30. Sullivan-Klose, T. H.; Ghanayem, B. I.; Bell, D. A.; Zhang, Z.-Y.; Kaminsky, L. S.; Shenfield, G. M.; Miners, J. O.; Birkett, D. J.; Goldstein, J. A. *Pharmacogenetics* **1996**, *6*, 341.
31. Hunter, W. N.; Kneale, G.; Brown, T.; Rabinovich, D.; Kennard, O. *J. Mol. Biol.* **1986**, *190*, 605.
32. Gao, Y.-G.; Robinson, H.; Sanishvili, R.; Joachimiak, A.; Wang, A. H.-J. *Biochemistry* **1999**, *38*, 16452.
33. Sargueil, B.; McKenna, J.; Burke, J. M. *J. Biol. Chem.* **2000**, *275*, 32157.
34. Okamoto, I.; Shohda, K.; Seio, K.; Sekine, M. *J. Org. Chem.* **2003**, *68*, 9971.
35. Puglisi, J. D.; Tinoco, I. In *Methods in Enzymology*; Dahlberg, J. E., Abelson, J. N., Eds.; Academic Press: San Diego, 1989; Vol. 180, pp 304–325.